JOC The Journal of Organic Chemistry

Article

Phenoxazine: A Privileged Scaffold for Radical-Trapping Antioxidants

Luke A. Farmer, Evan A Haidasz, Markus Griesser, and Derek A. Pratt

J. Org. Chem., **Just Accepted Manuscript** • DOI: 10.1021/acs.joc.7b02025 • Publication Date (Web): 08 Sep 2017

Phenoxazine: A Privileged Scaffold for Radical-Trapping Antioxidants

Luke A. Farmer, Evan A. Haidasz, Markus Griesser and Derek A. Pratt*

Department of Chemistry and Biomolecular Sciences, University of Ottawa, 10 Marie Curie Pvt., Ottawa, Canada.

*Corresponding author: Derek A. Pratt

Phone: 613-562-5800 Fax: 613-562-5170 E-mail: dpratt@uottawa.ca

TOC Graphic:

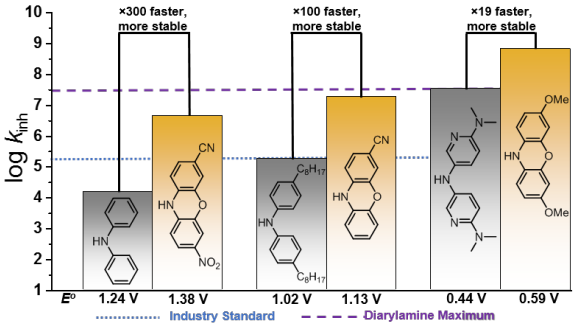

Abstract

Diphenylamines are widely used to protect petroleum-derived products from autoxidation. Their efficacy as radical-trapping antioxidants (RTAs) relies on a balance of fast H-atom transfer kinetics and stability to one electron oxidation by peroxidic species. Both H-atom transfer and one-electron oxidation are enhanced by substitution with electron-donating substituents, such as the S-atom in phenothiazines, another important class of RTA. Herein we report the results of our investigations of the RTA activity of the structurally-related, but essentially ignored, phenoxazines. We find that the H-atom transfer reactivity of substituted phenoxazines follows an excellent Evans-Polanyi correlation spanning $k_{inh}^{37\,°C}$ = 4.5 × 10^6 M^{-1} s^{-1} and N-H BDE = 77.4 kcal mol^{-1} for 3-CN,7-NO_2-phenoxazine to $k_{inh}^{37\,°C}$ = 6.6 × 10^8 M^{-1} s^{-1} and N-H BDE = 71.8 kcal mol^{-1} for 3,7-$(OMe)_2$-phenoxazine. The reactivity of the latter compound is the greatest of any RTA ever reported, and is likely to represent a reaction without enthalpic barrier since log *A* for this reaction is likely ~8.5. The very high reactivity of most of the phenoxazines studied required the determination of their kinetic parameters by inhibited autoxidations in the presence of a very strong H-bonding co-solvent (DMSO), which slowed the observed rates by up to two orders of magnitude by dynamically reducing the equilibrium concentration of (free) phenoxazine as an H-atom donor. Despite their remarkably high reactivity toward peroxyl radicals, the phenoxazines were found to be comparatively stable to one-electron oxidation relative to diphenylamines and phenothiazines (*E*° ranging from 0.59 V to 1.38 V *vs*. NHE). Thus, phenoxazines with comparable oxidative stability to commonly used diphenylamine and phenothiazine RTAs had significantly greater reactivity (by up to 2 orders of magnitude). Computations suggest that this remarkable balance in H-atom transfer kinetics and stability to one electron oxidation results from the ability of the bridging oxygen atom in phenoxazine to serve as both a π-electron donor to stabilize the aminyl radical and σ-electron acceptor to destabilize the aminyl radical cation. Perhaps most excitingly, phenoxazines have "non-classical" RTA activity – where they trap >2 peroxyl radicals each – *at ambient temperatures*.

Introduction.

Autoxidation, the radical-mediated chain reaction responsible for the spontaneous oxidation of hydrocarbons, is a ubiquitous process limiting the longevity of all living things and petroleum-derived materials. Radical trapping antioxidants (RTAs) compete with propagation of the autoxidation chain reaction by H-atom transfer to a chain-carrying peroxyl radical (Eq. 1).[1,2] Subsequent reaction of the RTA-derived radical with another chain-carrying peroxyl radical can inhibit a second chain reaction (Eq. 2). The efficacy of RTAs is largely governed by two metrics: the rate constant of the initial H-atom transfer reaction (the inhibition rate constant, k_{inh}) and the number of chains that are broken (the inhibition reaction stoichiometry, n).

$$\text{A-H} + \text{ROO}^{\bullet} \rightarrow \text{A}^{\bullet} + \text{ROOH} \qquad (1)$$

$$\text{A}^{\bullet} + \text{ROO}^{\bullet} \rightarrow \text{non-radical products} \qquad (2)$$

The among most widely-used RTAs are substituted phenols (e.g. butylated hydroxytoluene, BHT) and diphenylamines (e.g. alkylated diphenylamines, ADPAs). The reactivity of both classes of RTA obey good Evan-Polanyi relationships, where decreases in the phenolic O-H and aminic N-H bond dissociation enthalpies (BDEs) brought about by substitution of the aryl ring(s) with electron-donating groups (EDGs) give rise to larger k_{inh}.[3,4] The drop in BDE associated with the introduction of EDGs is accompanied by a drop in $E°$ and concomitant stability to one electron oxidation (by product hydroperoxides or O_2), which can lead to production of radical species rather than their trapping. Thus, achieving a balance of reactivity to H-atom transfer and stability to one-electron oxidation must be at the center of any RTA development strategy.

Although the structure-reactivity relationships in phenolic RTAs have been extensively studied, diphenylamines have been comparatively less well-investigated.[2,5–8] Of the existing work in this area, the careful thermochemical and kinetic studies of the reactivity of phenothiazines – diphenylamines (**1**) fused together by a central thiazine ring (**2**) – by Lucarini *et al* is particularly noteworthy.[6] They showed that phenothiazine has an N-H bond that is 6.5 kcal/mol weaker than in diphenylamine (78.2 *vs*. 84.7 kcal mol^{-1})[9] and a ~600-fold greater reactivity toward peroxyl radicals ($k_{inh} = 8.8 \times 10^6$ *vs*. 1.5×10^4 M^{-1} s^{-1} at 50 °C). Introduction of electron-donating methoxy substituents *para* relative to the aminic N-H further decreased the N-H BDE by 3.1 kcal mol^{-1} and

further increased k_{inh} by ~6-fold to 5.0×10^7 M^{-1} s^{-1} – the largest k_{inh} ever reported for a diarylamine.[10]

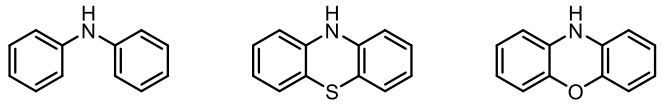

1 **2** **3**

In the same manuscript, Lucarini et al. presented corresponding data for phenoxazine (**3**), revealing that it possessed an even weaker N-H bond than phenothiazine (76.1 *vs*. 78.2 kcal mol^{-1})[9] and a correspondingly greater k_{inh} of 2.9×10^7 M^{-1} s^{-1}. No substituted phenoxazines were investigated. Perhaps most interestingly, while phenothiazine and the substituted phenothiazines that were investigated trapped ~2 peroxyl radicals each in inhibited autoxidations (i.e. $n \sim 2$), phenoxazine apparently trapped five. This was not explained. Moreover, although not pointed out at the time, despite its greater reactivity and stoichiometry, phenoxazine is (marginally) more stable to one-electron oxidation than phenothiazine (*vide infra*).[11] Hence, it would appear that phenoxazine is a privileged scaffold for RTA design and development. Herein we describe our efforts to characterize the structure-reactivity relationships in phenoxazines as RTAs, from which it is revealed that they are privileged structures with compelling prospects for real-world applications.

Results.

I. Exploiting Kinetic Solvent Effects to Clock the Fastest RTAs

The very high reactivity of phenoxazine to peroxyl radicals makes precise quantitation of the kinetics of the reaction challenging. Determination of inhibition rate constants of this magnitude (mid-10^7 $M^{-1}s^{-1}$) requires pushing the venerable inhibited autoxidation approach,[12,13] by which reaction progress is generally monitored by O_2 consumption, to its limit. Our own variation of the inhibited autoxidation approach,[14] in which a small amount of a highly absorbing co-substrate (PBD-BODIPY, Figure 1A) is added to the reaction mixture as a signal carrier, has an even lower limit ($k_{inh} \leq 10^7$ M^{-1} s^{-1}) due to the inherent reactivity of the co-substrate to peroxyl radicals (i.e. k_{BODIPY}= 2720 M^{-1} s^{-1} in styrene/chlorobenzene) and the maximum PBD-BODIPY concentration

that can be achieved without saturating the photomultipliers in a conventional spectrophotometer (10 μM). Indeed, phenoxazine completely inhibits PBD-BODIPY consumption in styrene autoxidations in chlorobenzene under standard conditions (black trace, Figure 1B), precluding determination of k_{inh} from the initial rate (Eq. 3) as in Figure 1C.[14]

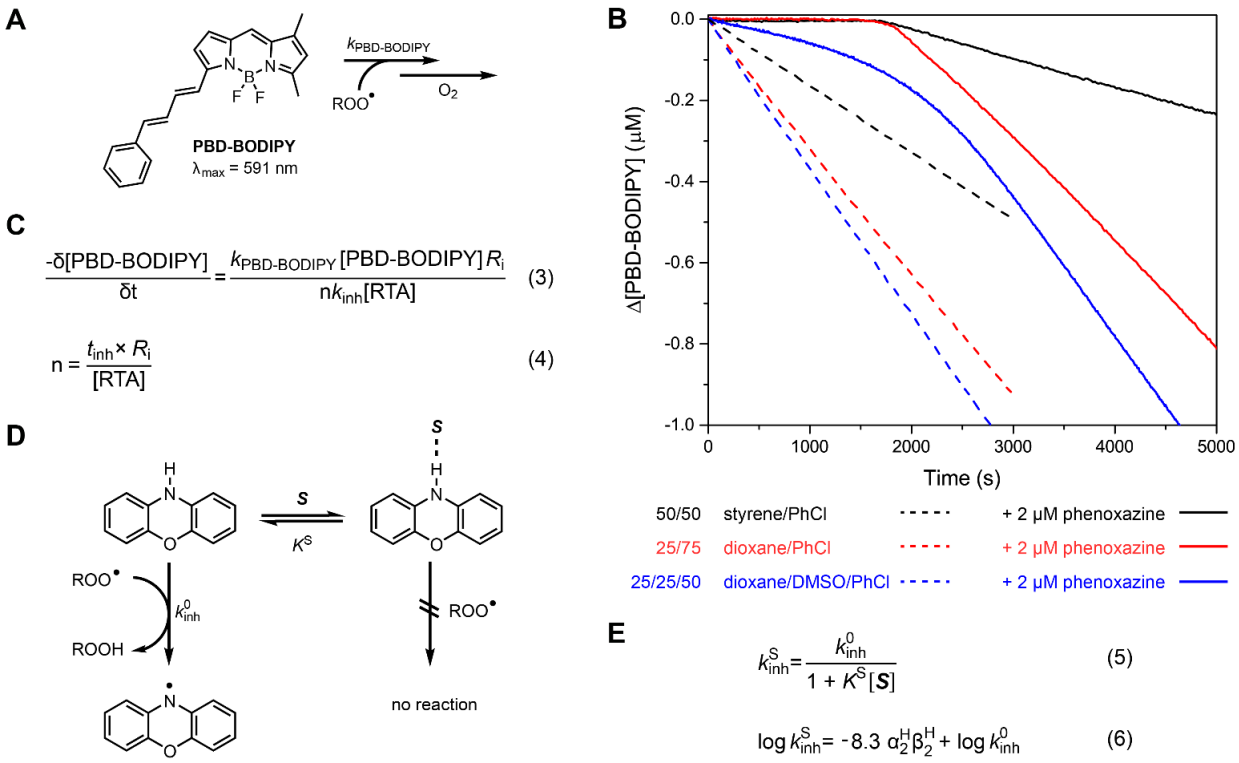

Figure 1. (**A**) PBD-BODIPY is used as a signal carrier in the autoxidation of styrene or 1,4-dioxane. (**B**) Co-autoxidation of styrene (4.3 M) and PBD-BODIPY (10 μM) in PhCl (black), 1,4-dioxane (2.9 M) in PhCl, and 1,4-dioxane (2.9 M) in 2:1 PhCl:DMSO initiated with 6 mM AIBN at 37 °C. Reaction progress was monitored at 591 nm (ε = 139 000 M^{-1} cm^{-1}), 587 nm (ε = 123 000 M^{-1} cm^{-1}), and 587 nm (ε = 118 200 M^{-1} cm^{-1}), respectively. (**C**) Rate constants (k_{inh}) and stoichiometries (n) for the reactions of inhibitors (RTAs) with chain-carrying peroxyl radicals can be determined from the initial rates and the duration of the inhibited periods as in Eqs. 3 and 4, respectively. (**D/E**) The equilibrium between 'free' RTA (illustrated by phenoxazine) and RTA participating in a 1:1 hydrogen-bond complex with arbitrary solvent *S*. Assuming the 1:1 complex does not react with peroxyl radicals, the kinetics of radical-trapping can be described as in Eq. 5 or Eq. 6.

In an attempt to circumvent this limitation, we exchanged styrene for an oxidizable substrate that would make H-bonds with phenoxazine (Figure 1D). This would lower the (free) concentration of phenoxazine in solution, thereby increasing the rate of the inhibited autoxidation such that it could be reliably measured. Ingold has shown that the kinetics of H-atom transfer reactions are retarded

in a wholly predictable fashion in H-bond accepting media, wherein the kinetics obey a pre-dissociation model as in Eq. 5 in Figure 1E.[15,16] Thus, if the equilibrium constant for H-bond formation between phenoxazine and the substrate (K_{HB}) is known, the rate constant for its reaction in the absence of strong H-bonding interactions (k_{inh}^{0}) can be derived from the observed rate constant (k_{inh}^{S}). This expression can be recast using Abraham's H-bond acidity (α_2^H)[17] and H-bond basicity (β_2^H)[18] parameters – which generally range from 0 to 1 – as in Eq. 6, a relationship that has been shown to hold for a variety of H-atom transfer reactions under a variety of conditions.

Thus, styrene was exchanged for dioxane as the oxidizable substrate. Dioxane is relatively easily oxidized (k_p = 0.5 M^{-1} s^{-1})[19] – ensuring that a free radical chain reaction is maintained in the autoxidation – and is also a good H-bond acceptor (β_2^H = 0.41).[18] However, using dioxane as the substrate was insufficient to increase the rate of the phenoxazine-inhibited autoxidation to a measurable level (Figure 1D). Hence, an even stronger H-bond acceptor was added as a co-solvent: DMSO (β_2^H = 0.78).[18] Upon doing so, the inhibited autoxidation clearly proceeded with a non-zero slope. Derivation of k_{inh} from the initial rate required determination of k_{BODIPY} in this solvent system (5900 M^{-1} s^{-1}, see Supporting Information), from which k_{inh}^{DMSO}= (5.3 ± 0.5) × 10^5 M^{-1} s^{-1} could be derived using Eq. 3.

To correct for the H-bonding interaction of phenoxazine with DMSO, thereby enabling derivation of the inherent reactivity of phenoxazine to peroxyl radicals, required that we determine α_2^H of phenoxazine and β_2^H of the solvent system. While exhaustive compilations of β_2^H parameters exist for a wide array of HBAs, our systems of interest consist of an amalgam of 2 or 3 potential HBDs. A direct approach to β_2^Hdetermination of a HBA would be to determine K_{HB} using quantitative IR spectroscopy in CCl_4.[20,21] We, however, opted for the ^{19}F NMR method devised by Taft et. al.,[22] where differences in the chemical shift of 4-fluorophenol and 4-fluoroanisole are related directly to K_{HB} (see the Supporting Information for further details). Using this method, an effective β_2^H of 0.35 was determined in 25% v/v dioxane in PhCl and β_2^H of 0.60 in 25% v/v dioxane with 25% v/v DMSO in PhCl.[23]

Similarly, the α_2^H of phenoxazine was determined by ^{1}H NMR. Abraham and co-workers have established that the chemical shift difference of the acidic proton of an HBD in $CDCl_3$ and d_6-DMSO obeys an excellent linear relationship with α_2^H (R^2 = 0.938 for 54 different species with a

total of 72 different protic functionalities).[24] Unfortunately, we found that phenoxazines are generally characterized by poorly resolved ^{1}H NMR spectra in $CDCl_3$. However, ^{1}H NMR spectra in benzene-d_6 are very well resolved and further, the chemical shift difference of the acidic protons of a variety of HBDs in this solvent relative to d_6-DMSO were also found to correlate very nicely to α_2^H according to the expression in Eq. 7 (R^2 = 0.972 for 11 different species ranging from α_2^H = 0.08 to 0.82, see ESI for the correlation).

$$\alpha_2^H = 0.134\,\Delta\delta_{DMSO-PhH} - 0.1087 \qquad (7)$$

The determination of $\Delta\delta_{DMSO-PhH}$ for phenoxazine affords α_2^H = 0.44 from this correlation. Using this value of α_2^H, β_2^H = 0.60 for the autoxidation solvent system and k_{inh} = (5.3 ± 0.5) × 10^5 M^{-1} s^{-1} determined from the inhibited autoxidation enables the derivation of k_{inh} = (3.9 ± 0.4) × 10^7 M^{-1} s^{-1} in chlorobenzene (β_2^H = 0.09),[18,25] which is in excellent agreement with the value obtained by Lucarini et al. in that solvent (2.9 × 10^7 M^{-1} s^{-1}).[6]

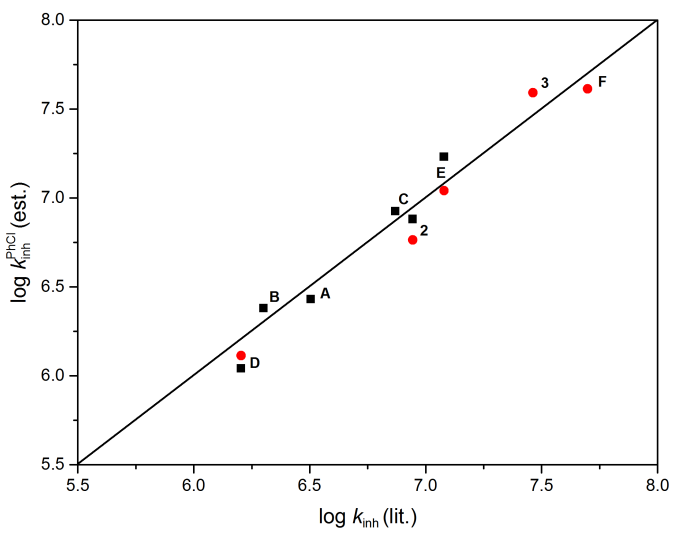

Figure 2. Inhibition rate constants derived from dioxane autoxidations in PhCl (black squares) or PhCl/DMSO (red circles) correlate very well with inhibition rate constants directly determined from styrene or 1-hexadecene autoxidations in PhCl. Representative inhibitors: PMC (**A**), 5-hydroxy-2-dimethylaminopyrimidine (**B**), 5-hydroxy-4,6-dimethyl-2-dimethylaminopyrimidine (**C**), 2-methylundecan-2-persulfide (**D**), phenothiazine (**2**), 3,7-di-tert-butylphenothiazine (**E**), 3,7-dimethoxyphenothiazine (**F**), phenoxazine (**3**). See ESI for full details.

In order to further validate the use of kinetic solvent effects to enable the determination of rate constants for very fast reactions of RTAs with peroxyl radicals, we carried out additional

autoxidations inhibited by phenothiazine, 3,7-dimethoxyphenothiazine and 3,7-di-*tert*-butylphenothiazine, as studied by Lucarini et al. by O_2 consumption in the inhibited autoxidation of styrene.[6] Moreover, since these compounds have largely similar HBD ability (α_2^H = 0.34-0.38), we also studied a few examples that were either excellent H-bond donors (two substituted pyrimidinols, α_2^H = 0.56/0.65)[26] or very poor ones (a hydropersulfide, α_2^H = 0.09).[27] The data is shown in Figure 2, along with the data for 2,2,5,7,8-pentamethylchroman-6-ol (PMC), a truncated form of α-tocopherol – Nature's premier RTA and an important benchmark compound in any RTA study.[28] Overall, the agreement with literature values determined directly in a non-H-bonding solvent (chlorobenzene) is excellent.

II. Structure-Activity Relationships in Phenoxazines as RTAs

With a methodology established to enable quantitative studies of very fast RTAs, the synthesis of a small library of substituted phenoxazines was carried out in order to evaluate the substituent effects on the parent structure's reactivity. 2-Trifluoromethylphenoxazine **4**, 3-trifluoromethylphenoxazine **5**, 2-*tert*-butylphenoxazine **6**, 3-*tert*-butylphenoxazine **7** and 3,7-di-*tert*-butylphenoxazine **8**, were each synthesized via intramolecular Cu-catalyzed Ullman-type couplings of the acetamido and bromo/iodo functionalities of corresponding diaryl ethers as in Scheme 1A.

2,4,6,8-Tetra-*tert*-butylphenoxazine **9** was synthesized by reduction of 2,4-di-*tert*-butyl-6-nitrophenol followed by self-condensation in acetic acid with zinc dust in a manner previously described.[29] 2,8-Di-*tert*-butylphenoxazine **10** was synthesized by the same method (Scheme 1B).

N,N-Diethyl-3-sulfonamidephenoxazine **11**, 3-cyanophenoxazine **12**, and 3-methoxy-7-nitrophenoxazine **13** were obtained by S_NAr of the appropriate o-aminophenol on a o-haloaryl/2-nitro-haloaryl (Scheme 1C). The formation of the diaryl ether followed by a Smiles rearrangement brokers an exclusive formation of the phenoxazine derivative wherein the substituent is located para to the reactive N-H.[30,31] 3-Nitrophenoxazine **14** and 3-cyano-7-nitrophenoxazine **15** were obtained by electrophilic nitration of 10-acetylphenoxazine[32] (with subsequent hydrolysis) and 3-cyanophenoxazine, respectively (Scheme 1D). 3-Methoxyphenoxazine **16** and 3,7-dimethoxyphenoxazine **17** were obtained by alkylation and then hydrolysis of hydroxy-*N*-

acetylphenoxazines derived from the reduction and acylation of phenoxazin-3-one and 7-hydroxy-phenoxazin-3-one, respectively (Scheme 1E).

Scheme 1. Preparation of Substituted Phenoxazines.

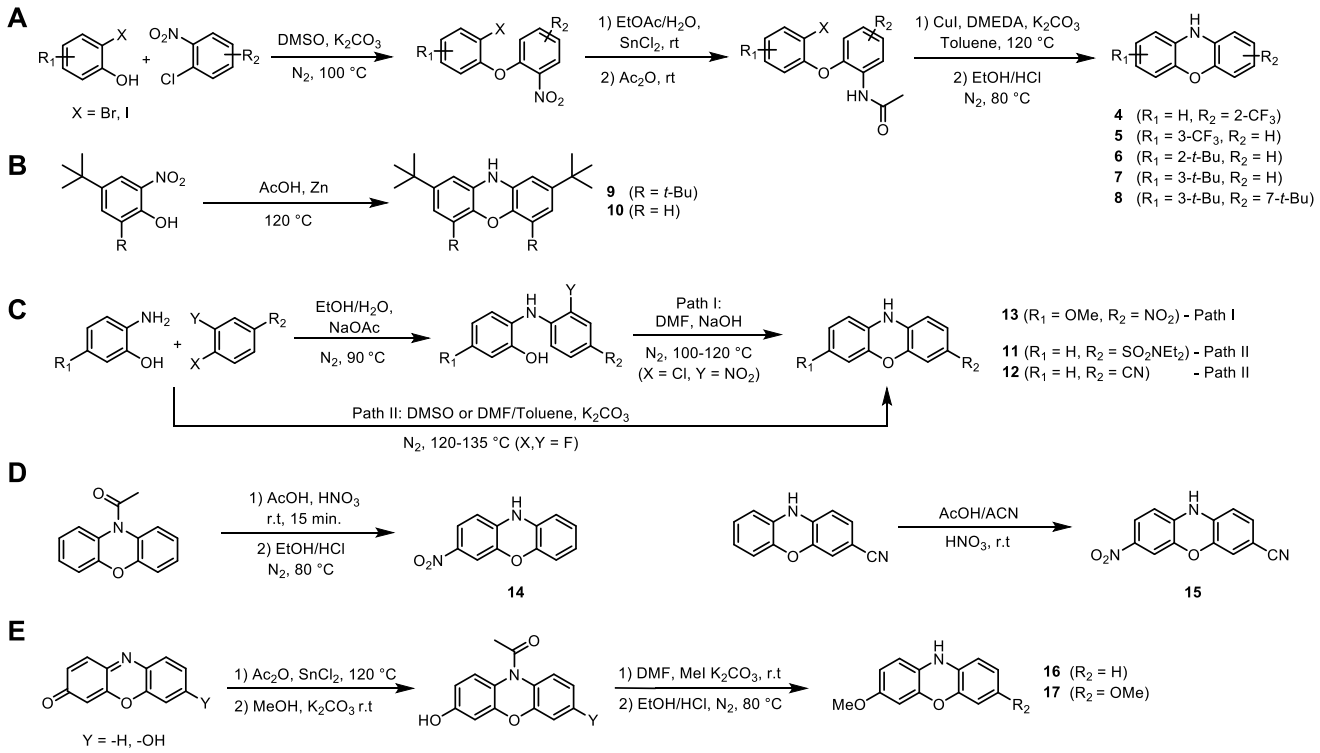

Inhibited autoxidations of dioxane in DMSO/PhCl were carried out as described above, with the choice of conditions dictated largely by the α_2^H values determined by NMR. The data is assembled in Table 1. As expected, phenoxazines with electron-withdrawing groups (EWGs) had substantially higher α_2^H parameters than phenoxazine, such that their k_{inh}^{PhCl} could be determined directly from inhibited autoxidations of dioxane sans DMSO whereas the phenoxazines substituted with electron-donating groups (EDGs) had marginally lower α_2^H – and were substantially more reactive than phenoxazine – so DMSO was added to the inhibited autoxidations. The quality of the α_2^H determinations for the substituted phenoxazines is reflected in the excellent correlation of these values with the corresponding σ_p^- substituent constants[33] (Figure 3A); expected since they are essentially partially dissociated Brønsted acids in the H-bonded complexes.

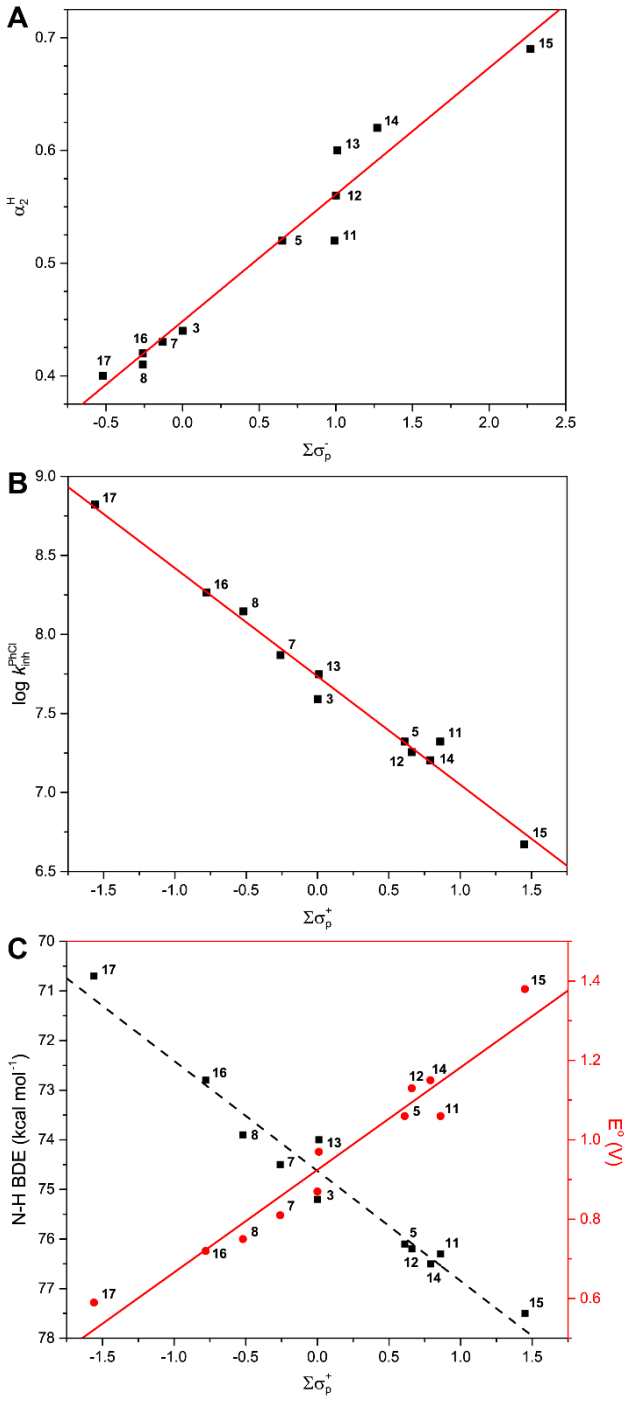

Figure 3. (**A**) Linear free energy relationship of $\Sigma\sigma_p^-$ and α_2^H for 3-substituted, or 3,7-disubstituted phenoxazines ($R^2 = 0.955$) (**B**) Linear free energy relationship of $\Sigma\sigma_p^+$ and $\log k_{inh}^{PhCl}$ for 3-substituted and 3,7-disubstituted phenoxazines ($\rho^+ = -0.68$, $R^2 = 0.982$) (**C**) Linear free energy relationship of $\Sigma\sigma_p^+$ and N-H BDE (black squares, $R^2 = 0.959$) and $\Sigma\sigma_p^+$ and E^o (red circles, $R^2 = 0.944$) for 3-substituted and 3,7-disubstituted phenoxazines.

The rate constants derived from the inhibited autoxidations span more than two orders of magnitude; the lowest determined for 3-CN,7-NO_2-phenoxazine ($4.5 \pm 0.1 \times 10^6$ M^{-1} s^{-1}) and the highest determined for 3,7-$(OMe)_2$-phenoxazine ($6.6 \pm 1.1 \times 10^8$ M^{-1} s^{-1}). In general, and as expected based on the kinetics of the reactions of other diarylamines with peroxyl radicals,[5,6,8] substitution with EDGs increase the rate and EWGs decrease the rate. In fact, the values of k_{inh} for the substituted phenoxazines correlate very well with the corresponding σ_p^+ substituent constants[33] – or sum of the substituent constants in the case of multiple substitutions – as is evident in Figure 3B. Also given in Table 1 are N-H BDEs that were calculated by the high-accuracy CBS-QB3 complete basis set methodology[34] and the standard potentials determined by cyclic voltammetry. As expected, both properties correlate well with $\Sigma\sigma_p^+$ (Figure 3C).[35]

III. Understanding the Superiority of Phenoxazine as an RTA

The CBS-QB3 calculations used to predict the N-H BDEs given in Table 1 were expanded to provide a view of the transition state structure for H-atom transfer from phenoxazine to peroxyl radicals (Figure 4A). The structure greatly resembles that of the reaction between diphenylamine and a peroxyl radical (Figure 4B) in that the proton is transferred roughly in the plane of the molecular framework, while the electron is delocalized in approximately perpendicular orbitals (i.e. the π-HOMO of phenoxazine and π*-SOMO of the peroxyl radical).[8] Thus, the reaction can be described as a proton-coupled electron transfer, where the proton and electron are exchanged between different pairs of orbitals.[7,8,27,36–39] The greater reactivity of phenoxazine is based on both enthalpic and entropic factors: the N-H bond is weaker, decreasing $\Delta H^{\ddagger}$ (0.8 vs. 5.1 kcal mol^{-1}), and the aryl rings are already fixed in optimal positions to maximize delocalization of the unpaired electron in the aminyl radical, minimizing the entropic cost ($\Delta S^{\ddagger}$ = -36.4 vs. -37.7 cal mol^{-1} for phenoxazine and diarylamine respectively).

In carrying out these calculations we also sought some insight into the origin of the relatively high $E°$ of phenoxazine (0.87 V *vs*. NHE) despite its low N-H BDE (76.1 kcal mol^{-1}) and corresponding high reactivity ($k_{inh} = 3 \times 10^7$ M^{-1} s^{-1}). To put this into context, diarylamines of similar or lower reactivity are generally characterized by $E°$ values which are ~0.4 V lower.[8] Of course, a fundamental difference between phenoxazine and diphenylamine is the planar structure of the latter – in both the starting material and the incipient radical and radical cation – which

should improve spin delocalization. Indeed, the N-H BDE and IP in 9,10-dihydroacridine are predicted to be 2.4 and 4.3 kcal mol^{-1} lower, respectively, than in diphenylamine. However, when the CH_2 bridge is replaced with an O-atom the predicted N-H BDE decreases by 11.2 kcal mol^{-1}, but this is accompanied by a decrease of only 8.7 kcal mol^{-1} in IP. The decrease in BDE upon inclusion of a heteroatom bridge in lieu of a methylene unit was anticipated, given that electron-donation from the heteroatom can better stabilize the electron poor aminyl radical by resonance. However, an even greater effect was expected on the ionization potential, given that the radical cation is inherently more electron poor than the amine. In order to eliminate the resonance contribution of the oxygen atom on the stability of the aminyl radical and/or cation, and focus only its inductive/field effect, we also calculated the N-H BDEs and IPs in piperidine and morpholine. Although the N-H BDEs are essentially identical, the oxygen atom clearly raises the IP of the amine. The inductive/field effect is even more obvious when the conformation of the piperidine and morpholine rings are constrained to be planar (as opposed to the minimum energy chair conformer); the IPs now differ by 8.3 kcal mol^{-1}, while the N-H BDEs remain essentially the same. A similar, but attenuated, trend exists in the corresponding sulfur compounds. These data are summarized in Figure 4E.

Table 1. Inhibition Rate Constants, α_2^H H-Bond Donor Parameters, Inhibition Stoichiometries, N-H Bond Dissociation Enthalpies and Oxidation Potentials for Substituted Phenoxazines.

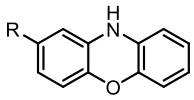

4 (R = CF_3)
6 (R = *t*-Bu)

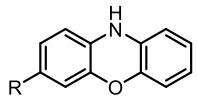

5 (R = CF_3) **12** (R = CN)
7 (R = *t*-Bu) **14** (R = NO_2)
11 (R = SO_2NEt_2) **16** (R = MeO)

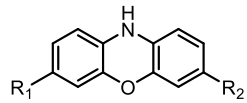

8 (R_1 = R_2 = *t*-Bu)
13 (R_1 = MeO, R_2 = NO_2)
15 (R_1 = NO_2, R_2 = CN)
17 (R_1 = R_2 = MeO)

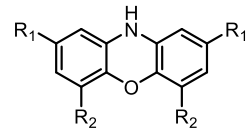

9 (R_1 = R_2 = *t*-Bu)
10 (R_1 = *t*-Bu, R_2 = H)

RTA	k_{inh}^{S} (M^{-1} s^{-1}) [a]	*n*	α_2^{H} [b]	k_{inh}^{PhCl} (M^{-1} s^{-1})	BDE (kcal mol^{-1}) [c]	E^{o} [d]
15[e]	$1.5 \pm 0.1 \times 10^5$	2.4 ± 0.1	0.69	$4.5 \pm 0.1 \times 10^6$	77.5	1.38
14[e]	$7.3 \pm 0.2 \times 10^5$	2.5 ± 0.1	0.62	$1.6 \pm 0.1 \times 10^7$	76.5	1.15
12[e]	$1.1 \pm 0.1 \times 10^6$	2.2 ± 0.2	0.56	$1.8 \pm 0.1 \times 10^7$	76.2	1.13
5[e]	$1.5 \pm 0.2 \times 10^6$	2.3 ± 0.1	0.53	$2.0 \pm 0.3 \times 10^7$	76.1	1.06
11[e]	$1.5 \pm 0.1 \times 10^6$	2.2 ± 0.1	0.53	$2.1 \pm 0.2 \times 10^7$	76.3	1.06
4[e]	$2.0 \pm 0.1 \times 10^6$	2.3 ± 0.1	0.51	$2.5 \pm 0.2 \times 10^7$	76.2	1.05
13[e]	$2.8 \pm 0.2 \times 10^6$	1.5 ± 0.1	0.60	$5.6 \pm 0.5 \times 10^7$	74.0	0.97
3[f]	$5.3 \pm 0.5 \times 10^5$	2.2 ± 0.1	0.44	$3.9 \pm 0.4 \times 10^7$	75.2	0.87
6[f]	$9.0 \pm 0.3 \times 10^5$	2.0 ± 0.1	0.43	$6.0 \pm 0.2 \times 10^7$	74.6	0.83
7[f]	$1.1 \pm 0.1 \times 10^6$	2.1 ± 0.1	0.43	$7.4 \pm 0.6 \times 10^7$	74.5	0.81
10[f]	$1.5 \pm 0.1 \times 10^6$	1.8 ± 0.1	0.43	$1.0 \pm 0.1 \times 10^8$	74.0	0.78
8[f]	$2.6 \pm 0.2 \times 10^6$	1.9 ± 0.1	0.41	$1.4 \pm 0.1 \times 10^8$	73.9	0.75
16[f]	$3.1 \pm 0.2 \times 10^6$	1.8 ± 0.1	0.42	$1.8 \pm 0.1 \times 10^8$	72.8	0.72
9[f]	$4.7 \pm 0.8 \times 10^6$	1.7 ± 0.1	0.39	$2.1 \pm 0.4 \times 10^8$	-	0.67
17[f]	$(1.3 \pm 0.2 \times 10^7)$[g]	1.4 ± 0.1	0.40	$(6.6 \pm 1.1 \times 10^8)$	70.7	0.59

[a]Rates of inhibition determined for 2 μM of inhibitor a minimum of three times. [b]Calculated from $\Delta\delta_{DMSO-PhH}$ of the relevant proton in the ^{1}H NMR spectrum in conjunction with Eq. 7. Spectra can be found in the ESI. [c]Calculated by CBS-QB3. [d]Values in V *vs.* NHE determined by cyclic voltammetry in acetonitrile. [e]k_{inh}^{PhCl} was calculated from k_{inh}^{Diox}. [f]k_{inh}^{PhCl} was calculated from k_{inh}^{DMSO}. [g]k_{inh}^{DMSO} was determined via kinetic modeling as described previously, see ref. 14.

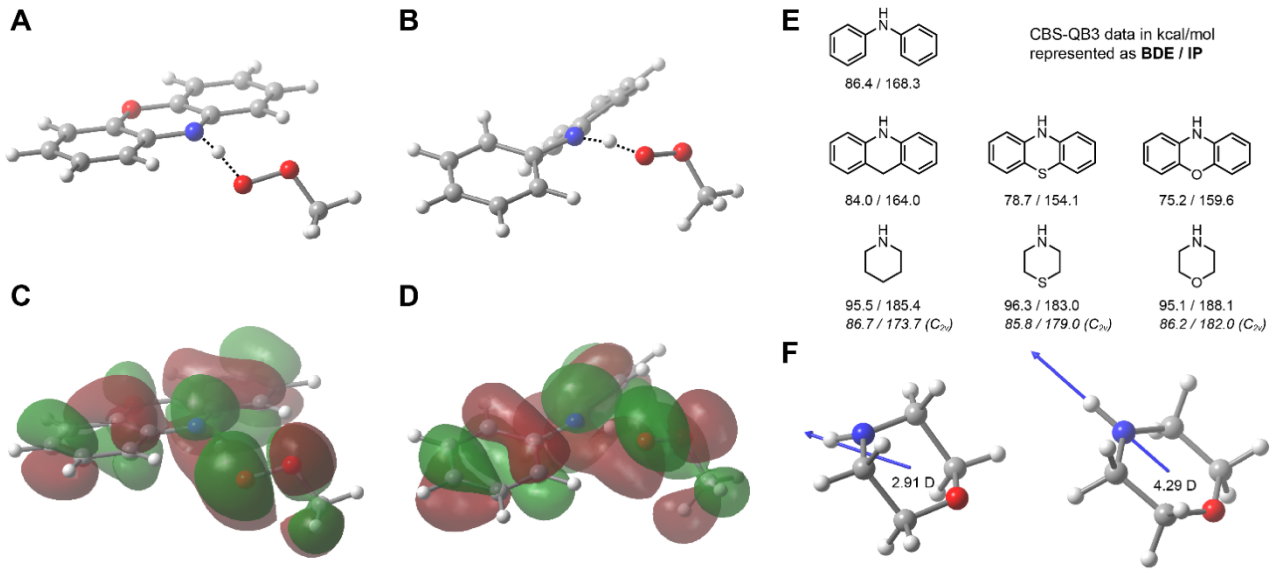

Figure 4. **(A/B)** Calculated TS structures of the reaction between a peroxyl radical (exemplified by methylperoxyl) and phenoxazine and diphenylamine. **(C/D)** Calculated singly occupied molecular orbitals of the TS. **(E)** CBS-QB3 calculated N-H BDEs and IPs of diphenylamine (top), 9,10-dihydroacridine, phenothiazine and phenoxazine (middle) and piperidine, thiomorpholine and morpholine (bottom). For piperidine, thiomorpholine and morpholine, data are presented for both the minimum energy conformation, as well as a planarized (C_{2v}) structure. **(F)** Calculated minimum energy and planarized structures of morpholine radical cation and molecular dipole moment vector.

Discussion

Phenothiazines, which are synthesized simply by treating diphenylamines with elemental sulfur in the presence of a catalytic oxidant (e.g. I_2), have been used as antioxidants since the 1950s.[40] Phenoxazines, despite being known to possess a weaker N-H bond and greater reactivity toward peroxyl radicals,[6] are not widely used – if at all. One consideration may be that they are not as conveniently prepared on industrial scale.[41] Another consideration may be that early reports suggested that phenoxazines were no more reactive than phenothiazines – at least at elevated temperatures – discouraging further investigation.[42] The more recent results of Lucarini et al.[6] strongly suggested to us that phenoxazines merit further investigation as RTAs; in particular, since they possess greater reactivity toward peroxyl radicals *and* greater stability to one-electron oxidation compared to phenothiazines.

The application of the spectrophotometric inhibited co-autoxidation approach[14] to the determination of the peroxyl radical-trapping kinetics of phenoxazines required slowing the inhibition reaction sufficiently to obtain a measurable rate for the inhibited part of the autoxidation. This was accomplished by the addition of a very strong H-bond accepting co-solvent (DMSO) to the reaction medium, precluding H-atom transfer from all but the tiny amount of non-H-bonded phenoxazine present at equilibrium. Although there are many examples of the utilization of the empirical equation derived by Ingold to estimate H-atom transfer rate constants in solvents of differing H-bond accepting ability (to which we refer as the Ingold-Abraham relationship, see Eq. 6),[21,43,44] we believe this to be the most extreme, given that DMSO is such an excellent H-bond acceptor (β_2^H = 0.78) and the very high inherent reactivity of some of the H-atom donors (i.e. in the absence of H-bonding interactions) are the fastest ever observed (k_{inh} up to mid 10^8 M^{-1} s^{-1}). As such, prior to our investigations of substituted phenoxazines, we first vetted the use of DMSO in combination with the Ingold-Abraham relationship by deriving the inhibition rate constants for other highly reactive RTAs whose kinetics had already been determined by oxygen consumption. The excellent agreement instilled confidence that data derived from PBD-BODIPY/dioxane co-autoxidations in DMSO are reliable.

The reactivity of the substituted phenoxazines was, as expected, impressive. At the low end, substitution at the 3- and 7- positions with cyano and nitro groups yields $k_{inh} = 4.5 \times 10^6$ M^{-1} s^{-1}; roughly one order of magnitude lower than phenoxazine. At the high end, substitution at the 3- and 7-positions with methoxy groups yields $k_{inh} = 6.6 \pm 1.1 \times 10^8$ M^{-1} s^{-1}; roughly one order of magnitude greater than phenoxazine. Phenoxazines substituted with single substituents were characterized by intermediate reactivity which correlated very well with the σ^+ Hammett-type electrophilic substituent constant to yield a strong linear free energy relationship (Figure 3B) whose negative reaction constant (ρ^+ = -0.68) is consistent with increasing electron-poorness of the aryl rings upon H-atom transfer from the phenoxazines to peroxyl radicals.

As far as we are aware, 3,7-dimethoxyphenoxazine is the most reactive radical-trapping antioxidant ever reported. In fact, it would appear that this reactivity is essentially the limit for these types of reactions. Previous work from our group had suggested that log A ~7.5 for the reactions of diarylamines with peroxyl radicals,[45] but the fact that the two aryl rings are fixed in phenoxazines reduces the entropy requirement to achieve the transition state (wherein optimal

delocalization of the unpaired electron in the incipient aminyl radical can occur). To a first approximation, these two bond rotations may contribute at most (since they are coupled) ½ log unit each to log *A*, suggesting that a value of ~8.5 is reasonable for phenoxazines. The only similarly reactive RTA reported to date is the 5-hydroxy-7-aza-2,3-dihydroindole shown in Chart 1, which was also believed to react with peroxyl radicals with essentially no enthalpic barrier (i.e. $E_a \sim 0$).[46]

Chart 1. Radical-trapping antioxidants with log k_{inh} ~ log A ~ 8.5.

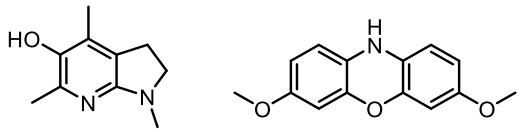

$k_{inh,\ PhCl}$ ($M^{-1}s^{-1}$)	(2.8 ± 1.8) × 10^8	(6.6 ± 1.1) × 10^8

Although they react more slowly, phenoxazines substituted with electron-withdrawing groups are arguably of greater practical interest. For example, the slowest phenoxazine we studied (3-CN, 7-NO_2) is ~300 fold more reactive than diphenylamine (compare k_{inh}^{PhCl} = 4.5 × 10^6 and 1.5 × 10^4 M^{-1} s^{-1}, respectively)[6] yet possesses greater stability to one-electron oxidation (compare $E°$ = 1.38 and 1.24 V *vs*. NHE, respectively).[47] Moreover, phenoxazines substituted with a single strong electron-withdrawing group (CN, NO_2, CF_3, SO_2NEt_2) were roughly 100-fold more reactive than the ADPAs used commercially (compare k_{inh}^{PhCl} ~2×10^7 versus 1.8 × 10^5 M^{-1} s^{-1},[8] respectively) while also being at least as stable to one electron oxidation ($E°$ >1 V *vs*. NHE). A particularly interesting compound is 3-methoxy-7-nitrophenoxazine. Since methoxy and nitro groups have the same magnitude of σ^+ constants, but of opposite sign (-0.78 and 0.79, respectively),[33] we expected their effects on the reactivity of phenoxazine to negate one another. However, this compound reacted 50% more quickly with peroxyl radicals than phenoxazine – and was characterized by a $E°$ value that was 100 mV greater – hence, the best of each substituent is contributed to these two key RTA parameters. The greater reactivity is consistent with the lower calculated N-H BDE in this compound compared to phenoxazine (74.4 vs. 75.2 kcal mol^{-1}), perhaps suggesting the role of captodative stabilization of the aminyl due to polarization across the two rings.

The unique combination of increased oxidative stability and increased H-atom transfer reactivity of phenoxazines relative to phenothiazines and diphenylamines is most clearly illustrated in Figure

5, where log k_{inh} is plotted versus $E°$ for the three types of arylamines. The three essentially parallel correlations reflect the fact that in compounds with a similar reactivity toward peroxyl radicals, the phenoxazine is considerably more stable to one-electron oxidation than phenothiazine, which is then more stable than the diphenylamine. Likewise, for compounds of the same oxidative stability, the phenoxazine is 5 to 10-fold more reactive than the phenothiazine, and even more so than the diphenylamine. The calculations described above provide good rationale for this; the π-donor ability of the oxygen atom in phenoxazine is responsible for the weaker N-H bond and larger k_{inh} compared to diphenylamine, but its σ-acceptor ability (electronegativity) minimizes the drop in $E°$. Although the sulfur atom in phenothiazine is also a good π-donor, such that it also possesses a weak N-H bond and large k_{inh}, since sulfur is less electronegative than oxygen it has a smaller effect on $E°$.

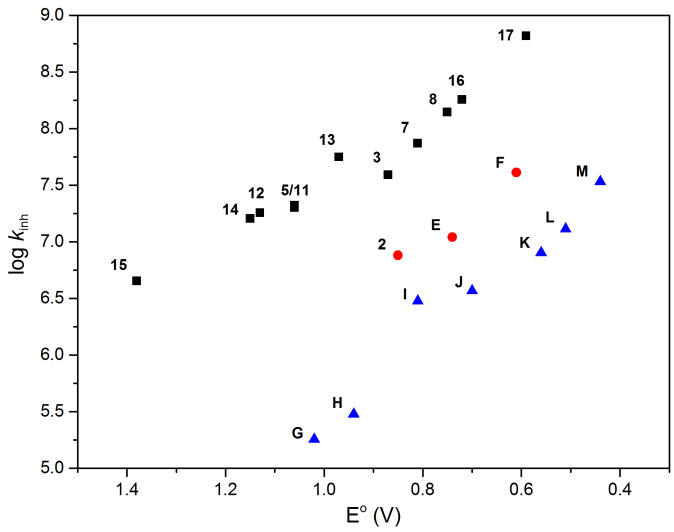

Figure 5. Inhibition rate constants of substituted phenoxazines (black), phenothiazines (red), and diarylamines (blue) plotted as a function of their oxidation potentials (E°). Representative inhibitors: 4,4'-dioctyldiphenylamine (**G**), 4-methoxydiphenylamine (**H**), N^2,N^2-dimethyl-N^5-phenylpyrimidine-2,5-diamine (**I**), 4,4'-dimethoxydiphenylamine (**J**), N^1,N^1-dibutyl-N^4-(pyrimidin-5-yl)benzene-1,4-diamine(**K**), 4-dimethylaminodiphenylamine (**L**), N^5-(6-(dimethylamino)pyridin-3-yl)-N^2,N^2-dimethylpyridine-2,5-diamine (**M**).[8] See ESI for structures.

One of the most interesting observations made by Lucarini et al. in their original work[6] was that styrene autoxidations inhibited by phenoxazine had inhibited periods that corresponded to the trapping of five (5!) peroxyl radicals. The foregoing dioxane/PBD-BODIPY co-autoxidations

were characterized by inhibited periods that correspond to $n \sim 2$, similar to phenols and other aminic antioxidants. However, when phenoxazine-inhibited co-autoxidations were carried out in styrene, a dramatic increase in the stoichiometric factor was observed (Figure 6A). Interestingly, the kinetic traces featured two distinct inhibited periods: an initial fully inhibited period ($t_{\mathrm{inh}}^{(1)} \sim$ 1700 s) corresponding to $n \sim 2$ and a secondary inhibited period ($t_{\mathrm{inh}}^{(2)} \sim 6700$ s) corresponding to an additional $n \sim 8$, for a total of $n \sim 10$. Moreover, the rate of the autoxidation beyond the second inhibited period remained retarded relative to the uninhibited rate. As far as we are aware, this level of radical-trapping capacity at ambient temperatures is unprecedented. It is noteworthy that two distinct inhibited phases (and subsequent retarded phase) in the phenoxazine-inhibited autoxidation of styrene were not reported by Lucarini et al.[6] This may be due to the significantly greater rate of initiation that they used to produce a non-zero inhibited autoxidation rate (necessary for them to derive k_{inh}), which would lead to a much less pronounced inflection point at $t_{\mathrm{inh}}^{(1)}$. It should also be pointed out that the previous measurements were made at 50°C.

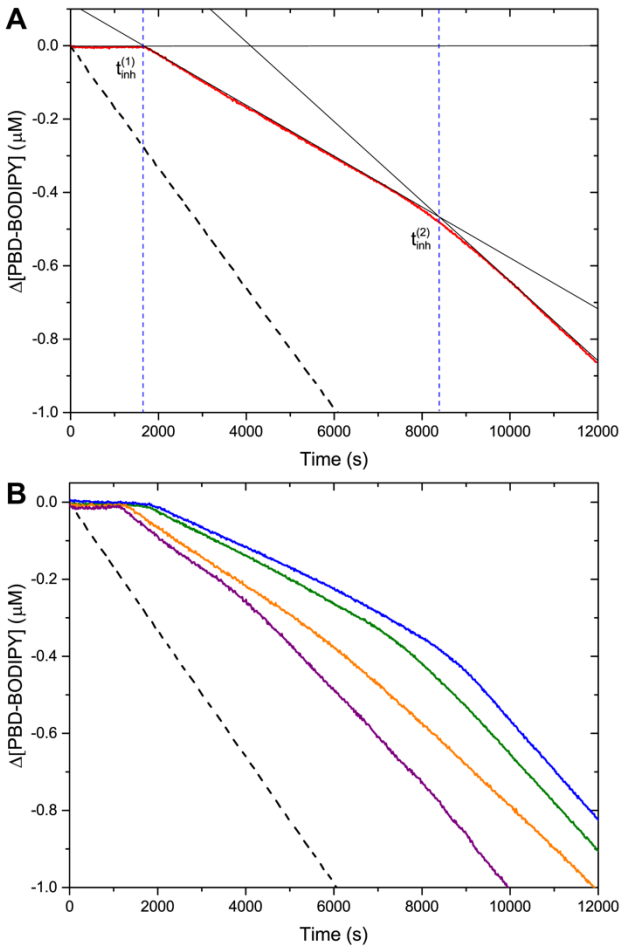

Figure 6. (**A**) Co-autoxidation of styrene (4.3 M) and PBD-BODIPY (10 uM) initiated by AIBN (6 mM) in PhCl at 37 ºC (black) and inhibited by 2 μM phenoxazine **3** (red, $n^{(1)} = 2.2 \pm 0.1$, $n^{(2)} = 8.0 \pm 1.9$). (**B**) Corresponding autoxidations inhibited by 2 μM of 3-cyanophenoxazine **12** (blue, $n^{(1)} = 2.4 \pm 0.1$, $n^{(2)} = 9.4 \pm 0.5$), 3-(N,N-diethylsulfonamide)-phenoxazine **11** (green, $n^{(1)} = 2.3 \pm 0.1$, $n^{(2)} = 8.1 \pm 0.6$), 3-tert-butylphenoxazine **7** (orange, $n^{(1)} = 1.9 \pm 0.3$, $n^{(2)} = 6.7 \pm 1.4$) and 3-methoxyphenoxazine **16** (violet, $n^{(1)} = 1.8 \pm 0.3$, $n^{(2)} = 3.9 \pm 0.5$).

In addition to the striking substrate-dependence of this "non-classical" RTA behavior, we also found that the rate of the secondary inhibited period is largely independent of the structure of the phenoxazine ($k_{inh}^{secondary} = 5.1 \pm 0.1 \times 10^5$ $M^{-1}s^{-1}$ for **3**, $5.3 \pm 0.4 \times 10^5$ $M^{-1}s^{-1}$ for **7**, $6.2 \pm 0.1 \times 10^5$ $M^{-1}s^{-1}$ for **11**, $7.2 \pm 0.3 \times 10^5$ $M^{-1}s^{-1}$ for **12**, and $4.3 \pm 0.5 \times 10^5$ $M^{-1}s^{-1}$ for **16**). Representative examples are shown in Figure 6B, which features data for styrene autoxidations inhibited by both electron-rich (methoxy- or *tert*-butyl-substituted) and electron-poor (sulfonamide- or cyano-substituted) phenoxazines. The major difference between these data sets is the difference in the lengths of both the primary and secondary inhibited periods, with the more electron-rich

phenoxazines giving rise to noticeably shorter overall inhibited periods, such that the overall *n* decreases upon increasing electron-richness: 11.6 (3-CN), 10.4 (3-Et_2NSO_2), 10.2 (3-H), 8.6 (3-*t*-Bu), 5.7 (3-OMe). This is presumably due to the increased oxidative lability of the phenoxazines along this series, which depletes the RTA and generates radicals rather than traps them.

Non-classical ($n > 2$) RTA activity of diarylamines is well known, but only at elevated temperatures (i.e. >100 °C)[2] – such as those experienced by engine oil lubricants, rubbers and plastics to which ADPAs are added. The need for elevated temperatures is easily understood upon consideration of the accepted mechanism for the catalytic activity of ADPAs, shown in Scheme 2.[48] Following the initial H-atom transfer to a peroxyl radical, the diphenylaminyl radical reacts with a second peroxyl radical to form a nitroxide. The nitroxide then combines with an alkyl radical to form an alkoxyamine, that can undergo rate-limiting fragmentation to reform the ADPA. The fragmentation requires cleavage of the N-O bond either by homolysis/disproportionation or a concerted retro-carbonyl-ene pericyclic process,[49] both of which do not operate on the timescale of the inhibited autoxidations shown in Fig. 6 at 37 °C ($k \sim 3 \times 10^{-9}$ s^{-1}).[49] Of course, the rate may increase if the aminyl radical formed upon N-O homolysis is significantly more stable, as is the aminyl derived from phenoxazine. However, the difference in the aminyl radical stabilities – which can be estimated from the difference in the N-H BDEs between ADPAs (~82 kcal mol^{-1}) and phenoxazine (~76 kcal mol^{-1}) – is too little to increase the rate of fragmentation of the putative alkoxyamine sufficiently to account for the secondary inhibition observed in the styrene autoxidations (Figure 6).[50] Moreover, the rates during the secondary inhibited periods to which the "non-classical" RTA activity is attributed are almost independent of the structure of the phenoxazine – inconsistent with N-O homolysis to yield aminyl radicals of significantly different stability being rate-determining (i.e. the difference in N-H BDEs of the cyano and methoxy substituted phenoxazines is 3.2 kcal/mol). Clearly, another mechanism must operate – and must do so in styrene, but not dioxane. Efforts to elucidate this mechanism continue in our laboratories.

Scheme 2. Mechanism of Diarylamine RTAs at Elevated Temperatures.

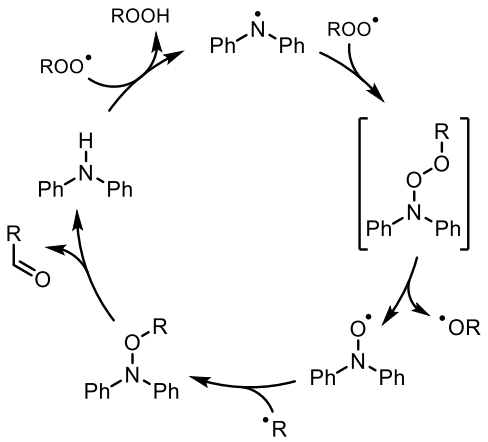

Given the higher reactivity, radical-trapping capacity and oxidative stability of phenoxazines compared to other aminic RTAs, it will be interesting to see how they compare in industrially-relevant contexts. Moreover, given that even the least reactive phenoxazine studied here is still more reactive than α-TOH, the most biologically-active form of Vitamin and Nature's premier RTA (k_{inh} = 3.2 × 10^6 M^{-1} s^{-1}),[28] it would be interesting to see if these compounds have any biological activity. Again, this is particularly interesting given that α-TOH is comparatively easy to oxidize ($E°$ = 0.93 V).[51] Indeed, we recently found that phenoxazine is the most potent inhibitor of lipid autoxidation driven cell death (also called ferroptosis) ever reported,[52] corroborating an earlier study that suggested that phenoxazine was a potent neuroprotectant.[53] Thus, some of the compounds described here may provide leads toward potential preventive and/or therapeutic agents for degenerative conditions wherein lipid autoxidation has been implicated.

Conclusions

Application of the kinetic solvent effect model of Ingold has enabled quantitation of the kinetics of the reactions of substituted phenoxazines with peroxyl radicals (k_{inh}). The addition of DMSO as a co-solvent to dioxane autoxidations suppressed the reactivity of phenoxazines by up to two orders of magnitude, thereby enabling derivation of their inhibition rate constants under more relevant (i.e. non-H-bonding) conditions via the Ingold-Abraham relationship. The reliability of this approach can be appreciated explicitly by the accuracy of the derived rate constants with

respect to previously characterized RTAs, as well as implicitly based on the strong linear correlation between σ_p^+ and log k_{inh}^{PhCl} for the newly studied substituted phenoxazines.

The reactivity of the phenoxazines spanned 4.5×10^6 M^{-1} s^{-1} for 3-CN,7-NO_2-phenoxazine to 6.6×10^8 M^{-1} s^{-1} for 3,7-$(OMe)_2$-phenoxazine. The reactivity of the latter compound is the greatest of any RTA ever reported, and is likely to represent a reaction without enthalpic barrier since log *A* for this reaction is likely ~8.5. Linear free energy relationships observed between the inhibition rate constants, standard potentials and N-H bond strengths of phenoxazines parallel those of substituted diarylamines and phenothiazines. However, with respect to the other classes of aminic RTAs, the substituted phenoxazines are decisively privileged since compounds of similar oxidative stability (quantified by E^o) are orders of magnitude more reactive to peroxyl radicals. The results of computations account for this, by indicating that the heteroatom bridge in phenoxazines (and to a lesser extent, phenothiazines) stabilizes the aminyl radical by electron donation resonance while destabilizing the aminyl radical cation by electron withdrawal by induction. Perhaps most interestingly, we confirm the once-reported non-classical RTA behavior of phenoxazine at ambient temperatures, and show that 1) it is dependent on the rate of initiation of autoxidation, 2) is only weakly dependent on the electronic characteristics of the phenoxazine, and 3) is dependent on the substrate undergoing autoxidation. The precise mechanism of this non-classical RTA behavior remains unknown.

Experimental

General Methods All chemicals and solvents were purchased from commercial suppliers unless otherwise indicated. ^{1}H, ^{13}C, and ^{19}F NMR spectra were recorded on either a 300 or 400 MHz instrument. UV-visible spectra and associated kinetics were measured with a spectrophotometer equipped with a temperature controller unit and a thermostated 6 × 6 multicell holder. Styrene was washed thrice with 1 M NaOH, once with water and then dried with $MgSO_4$ prior to distillation under reduced pressure at 50 °C. Thereafter, it was passed through a column of silica and stored at -20 °C for up to 4 days. Immediately prior to use, it was passed through a column filled with 2/3 basic alumina (bottom) and 1/3 silica (top). 3-Cyanophenoxazine,[30] 10-acetylphenoxazine,[54] 3,7-dihydroxy-10-acetylphenoxazine,[55] phenoxazone,[56] *N*-[2-(4-(*tert*-butyl)-2-

iodophenoxy)phenyl]acetamide,[57] 5-hydroxy-2-dimethylaminopyrimidine,[26b] 5-hydroxy-4,6-dimethyl-2-dimethylaminopyrimidine,[26b] 2-methylundecan-2-persulfide,[27] 3,7-di-*tert*-butylphenothiazine,[58] and 3,7-dimethoxy-phenothiazine[59] were prepared according to previously reported procedures.

2-Iodo-5-*tert*-butylphenol. 3-*tert*-Butylphenol (2.55 g, 17.0 mmol), potassium iodide (2.78 g, 16.8 mmol), and NaOH (0.68 g, 17.0 mmol) were dissolved in MeOH (46 mL) under stirring, cooled with an ice bath. Approximately 22 mL of 6% sodium hypochlorite solution (bleach) was added drop wise over an hour until the potassium iodide was consumed. On completion, the reaction mixture was poured into water, the aqueous mixture extracted thrice with EtOAc. The organic phase washed twice with water, dried over $MgSO_4$, filtered and the solvent removed under reduced pressure. The residue was purified by column chromatography (9:1, hexanes:EtOAc) to render the product as a clear oil, which quickly changed to a reddish color and under cooling in a freezer, formed prismatic crystals (3.27 g, 69%). ^{1}H NMR (400 MHz; $CDCl_3$): δ 7.56 (d, J = 8.3 Hz, 1H), 7.05 (d, J = 2.3 Hz, 1H), 6.74 (dd, J = 2.3, 8.3 Hz, 1H), 5.20 (br, 1H), 1.30 (s, 9H). Spectra were consistent with previous reports.[60]

4-(*tert*-Butyl)-2-chloronitrobenzene. 5-(*tert*-Butyl)-2-nitroaniline (0.98 g, 5.0 mmol) was dissolved in 20 mL concentrated HCl at room temperature under vigorous stirring, to which sodium nitrite (0.42 g, 6.1 mmol) in a minimum of water was added slowly. The suspension was allowed to stir for 1 hour at room temperature. Copper(I) chloride (50 mg, 0.5 mmol) dissolved in a small amount of HCl was added slowly and the mixture heated to 100 °C for 1 hour. The reaction mixture was poured into water and the aqueous mixture extracted thrice with Et_2O. The organic phase was washed twice with water, dried over $MgSO_4$, filtered and the solvent removed under reduced pressure. The orange residue (0.33 g) was largely the desired product based on crude spectra (*see ESI*), though attempts to completely isolate the product from the side products by column chromatography were unsuccessful, so the crude product was used without further purification.

4-(*tert*-Butyl)-1-iodo-2-(2-nitrophenoxy)benzene. 2-Iodo-5-*tert*-butylphenol (2.79 g, 10.0 mmol) and 2-chloronitrobenzene (1.58 g, 10.0 mmol) were dissolved in DMSO (15 mL) to which K_2CO_3 was added (2.81 g, 20.3 mmol) and the reaction mixture was placed under a N_2 atmosphere. With vigorous stirring, the reaction was heated to 100 °C overnight. The reaction mixture was

poured into water and extracted thrice with EtOAc. The organic phase was washed twice with water, dried over $MgSO_4$, filtered and the solvent removed under reduced pressure. The product was purified by column chromatography (9:1, pet. ether:Et_2O) to render a clear oil (2.92 g, 73%). ^{1}H NMR (300 MHz; $CDCl_3$): δ 8.01 (dd, *J* = 1.7, 8.0 Hz, 1H), 7.79 (d, *J* = 8.3 Hz, 1H), 7.51-7.45 (m, 1H), 7.21-7.16 (m, 1H), 7.09 (d, *J* = 2.2 Hz, 1H), 7.03 (dd, *J* = 2.2, 8.3 Hz, 1H), 6.78 (dd, *J* = 1.1, 8.3 Hz, 1H), 1.28 (s, 9H). ^{13}C NMR (75 MHz; $CDCl_3$): δ 154.4, 154.2, 150.7, 139.6, 134.1, 125.9, 124.5, 122.6, 118.6, 118.2, 85.4, 34.8, 31.1. HRMS (EI, magnetic sector) m/z: M+ Calcd for $C_{16}H_{16}INO_3$ 397.01749, found 397.01553.

1-(2-Bromophenoxy)-2-nitro-4-(trifluoromethyl)benzene. Same general procedure where 2-bromophenol (1.75 g, 10.0 mmol) and 4-chloro-3-nitrobenzotrifluoride (2.26 g, 10.0 mmol) were heated in DMSO with K_2CO_3. The resulting oil (3.49 g; 97%) was used in the subsequent reaction without further purification. ^{1}H NMR (400 MHz; $CDCl_3$): δ 8.28 (d, 2.3 Hz, 1H), 7.72-7.69 (m, 2H), 7.45-7.40 (m, 1H), 7.24-7.18 (m, 2H), 6.87 (d, 8.8Hz, 1H). ^{13}C NMR (101 MHz; $CDCl_3$): δ 153.0, 150.7, 139.6, 134.5, 130.9 (q, $J_{C\text{-}F}$ = 3.3Hz), 129.4, 127.7, 125.1 (q, $J_{C\text{-}F}$ = 34.9 Hz), 123.7 (q, $J_{C\text{-}F}$ = 4.0 Hz), 122.8 (q, $J_{C\text{-}F}$ = 272.2 Hz), 122.6, 118.2, 115.8. ^{19}F NMR (376 MHz, $CDCl_3$): δ -63.40. HRMS (EI, magnetic sector) m/z: M+ Calcd for $C_{13}H_7BrF_3NO_3$ 360.95614, found 360.95252.

1-Iodo-2-(2-nitrophenoxy)-4-(trifluoromethyl)benzene. Same general procedure where 2-iodo-5-trifluoromethylphenol (1.62 g, 5.6 mmol) and 2-chloronitrobenzene (0.66 g, 4.2 mmol) were heated in DMSO with K_2CO_3. Attempts to completely isolate the product from the side products by column chromatography were unsuccessful, so the crude product was used without further purification. See ESI for crude ^{1}H and ^{13}C NMR spectra. HRMS (EI, magnetic sector) m/z: M+ Calcd for $C_{13}H_7IF_3NO_3$ 408.94227, found 408.94262.

4-(*tert*-Butyl)-2-(5-(tert-butyl)-2-iodophenoxy)-1-nitrobenzene. Same general procedure where 2-iodo-5-tert-butylphenol (0.42 g, 1.5 mmol) and 4-(*tert*-butyl)-2-chloronitrobenzene (0.32 g, 1.5 mmol) were heated in DMSO with K_2CO_3. The product was purified by column chromatography (9:1, pet. ether:Et_2O) to afford a white solid (0.34 g, 50%). ^{1}H NMR (400 MHz; $CDCl_3$): δ 7.98 (d, *J* = 8.6 Hz, 1H), 7.79 (dd, *J* = 0.6, 7.9 Hz, 1H), 7.22 (dd, *J* = 2.0, 8.6 Hz, 1H), 7.00-6.97 (m, 2H), 6.86 (d, *J* = 2.0 Hz, 1H), 1.26 (s, 9H), 1.24 (s, 9H). ^{13}C NMR (101 MHz; $CDCl_3$): δ 159.0,

154.7, 154.1, 150.0, 139.6, 138.1, 125.9, 123.6, 120.2, 117.1, 116.5, 84.6, 35.4, 34.8, 31.0, 30.8. HRMS (EI, magnetic sector) m/z: M+ Calcd for $C_{20}H_{24}INO_3$ 453.08009, found 453.08007.

N-(2-(5-(tert-butyl)-2-iodophenoxy)phenyl)acetamide. 4-(*tert*-Butyl)-1-iodo-2-(2-nitrophenoxy)benzene (2.88 g, 7.2 mmol) and 5 equivalents of $SnCl_2$ (6.83 g, 36.0 mmol) were dissolved in EtOAc along with 10 equivalents of H_2O (1.3 mL). The reaction stirred at room temperature overnight, then was poured into water and extracted thrice with EtOAc. The organic phase was washed twice with water, dried over $MgSO_4$, filtered and the solvent removed under reduced pressure. The residue was dissolved in neat acetic anhydride (3.4 mL) and allowed to stir overnight. The reaction was quenched with saturated Na_2CO_3 solution and extracted thrice with EtOAc. The organic phase was washed once with water, dried over $MgSO_4$, filtered and the solvent removed under reduced pressure. The resulting product (2.65 g, 90%) was further purified by column chromatography (4:1, pet. ether:Et_2O) to afford a colorless oil. ^{1}H NMR (300 MHz; $CDCl_3$): δ 8.45 (dd, J = 1.3, 8.1 Hz, 1H), 7.84 (br, 1H), 7.79 (d, J = 8.3 Hz, 1H), 7.15-7.09 (m, 1H), 7.03-6.96 (m, 3H), 6.69 (dd, J = 1.4, 8.1 Hz, 1H), 2.23 (s, 3H), 1.27 (s, 9H). ^{13}C NMR (75 MHz; $CDCl_3$): δ 168.3, 154.7, 154.3, 145.3, 139.3, 129.0, 123.73, 123.70, 121.0, 117.5, 115.9, 104.5, 85.0, 34.8, 31.1, 25.0. HRMS (EI, magnetic sector) m/z: M+ Calcd for $C_{18}H_{20}INO_2$ 409.05387, found 409.05556.

N-(2-(2-bromophenoxy)-5-(trifluoromethyl)phenyl)acetamide. Same general procedure where 1-(2-bromophenoxy)-2-nitro-4-(trifluoromethyl)benzene (3.47 g, 9.6 mmol) is reduced with $SnCl_2$, then acetylated in neat acetic anhydride. The resulting solid (3.20 g, 90%) was used in the subsequent reaction without further purification. ^{1}H NMR (400 MHz; $CDCl_3$): δ 8.82 (br, 1H), 7.94 (br, 1H), 7.70 (dd, J = 1.6, 8.0 Hz, 1H), 7.39 (ddd, J = 1.6, 8.0, 8.0 Hz, 1H), 7.24-7.21 (m, 1H), 7.19-7.15 (m, 1H), 7.12 (dd, J = 1.5, 8.1 Hz, 1H), 6.68 (d, J = 8.5 Hz, 1H), 2.27 (s, 3H). ^{13}C NMR (101 MHz; $CDCl_3$): δ 168.5, 151.4, 147.7, 134.3, 129.2, 129.0, 126.9, 125.8 (q, $J_{C\text{-}F}$ = 33.0 Hz), 123.88 (q, 272.2 Hz), 122.05, 120.69 (q, $J_{C\text{-}F}$ = 3.7 Hz), 117.94 (q, $J_{C\text{-}F}$ = 3.7 Hz), 115.54, 114.90, 24.89. ^{19}F NMR (376 MHz, $CDCl_3$): δ -63.11. HRMS (EI, magnetic sector) m/z: M+ Calcd for $C_{15}H_{11}BrF_3NO_2$ 372.99253, found 372.99317.

N-(2-(2-iodo-5-(trifluoromethyl)phenoxy)phenyl)acetamide. Same general procedure where 1-iodo-2-(2-nitrophenoxy)-4-(trifluoromethyl)benzene (0.41 g, 1.0 mmol) is reduced with $SnCl_2$, then acetylated in neat acetic anhydride. The isolated crude solid was recrystallized from hexanes

to afford pure white needles (0.21 g, 50%); mp 114-115 °C; ^{1}H NMR (400 MHz; $CDCl_3$): δ 8.48 (d, *J* = 8.4 Hz, 1H), 8.03 (d, *J* = 8.2 Hz, 1H), 7.69 (b, 1H), 7.23-7.08 (m, 4H), 6.80 (dd, *J* = 1.0, 8.2 Hz, 1H), 2.22 (s, 3H). ^{13}C NMR (101 MHz; $CDCl_3$): δ 168.3, 155.9, 144.3, 140.7, 132.6 (q, J_{C-F} = 33.4 Hz), 129.5, 125.2, 124.1, 123.2 (q, J_{C-F} = 272.5 Hz), 122.3 (q, J_{C-F} = 3.7 Hz), 121.5, 117.3, 115.3 (q, J_{C-F} = 3.7 Hz), 92.8, 24.9. ^{19}F NMR (376 MHz, $CDCl_3$): δ -64.09. HRMS (EI, magnetic sector) m/z: M+ Calcd for $C_{15}H_{11}F_3INO_2$ 420.97866, found 420.97881.

N-(4-(*tert*-butyl)-2-(5-(tert-butyl)-2-iodophenoxy)phenyl)acetamide. 4-(*tert*-Butyl)-2-(5-(*tert*-butyl)-2-iodophenoxy)-1-nitrobenzene (0.71 g, 1.6 mmol) and 5 equivalents of $SnCl_2$ dihydrate (1.52 g, 8.0 mmol) were dissolved in EtOAc. The reaction was stirred at room temperature overnight, then poured into water and extracted thrice with Et_2O. The organic phase was washed twice with water, dried over $MgSO_4$, filtered and the solvent removed under reduced pressure. The residue was dissolved in THF (10 mL) to which were added triethylamine (0.30 mL, 2.1 mmol) and acetyl chloride (0.13 mL, 1.8 mmol). The mixture was stirred overnight, then poured into water and extracted twice with Et_2O. The organic phase was washed twice with water, dried over $MgSO_4$, filtered and the solvent removed under reduced pressure. The resulting product (0.68 g, 91%) was further purified by column chromatography (9:1 hexanes:EtOAc) to afford a colorless oil. ^{1}H NMR (300 MHz; $CDCl_3$): δ 8.32 (d, *J* = 8.6 Hz, 1H), 7.78 (d, *J* = 8.6 Hz, 1H), 7.72 (br, 1H), 7.16 (dd, *J* = 2.2, 8.6 Hz, 1H), 6.97-6.93 (m, 2H), 6.86 (d, *J* = 2.2 Hz, 1H), 2.19 (s, 3H), 1.24 (s, 18H). ^{13}C NMR (75 MHz; $CDCl_3$): δ 168.2, 155.0, 154.0, 147.3, 144.4, 139.2, 126.8, 122.9, 120.9, 120.8, 115.7, 114.6, 84.0, 34.8, 34.5, 31.2, 31.0, 24.8. HRMS (EI, magnetic sector) m/z: M+ Calcd for $C_{22}H_{28}INO_2$ 465.11647, found 465.11865.

2-*tert*-Butyl-10-acetylphenoxazine. Into a N_2 flushed sealed tube were added N-(2-(4-(*tert*-butyl)-2-iodophenoxy)phenyl)acetamide (3.42 g, 8.3 mmol), K_2CO_3 (2.32 g, 16.8 mmol), copper(I) iodide (86 mg, 0.05 eq.), N,N'-dimethylethylenediamine (90 μL, 0.10 eq.), and toluene (35 mL). The reaction mixture was heated to 120 °C for at least 10 hours under vigorous stirring, After completion, the reaction mixture was diluted with dichloromethane and passed through a plug of silica, after which the solvent was removed under reduced pressure. The crude product was purified by column chromatography (3:1, hexanes:EtOAc) to render 2-*tert*-butyl-10-acetylphenoxazine as an off-white solid (1.65 g, 71%). ^{1}H NMR (400 MHz; $CDCl_3$): δ 7.53 (d, *J*

= 7.9 Hz, 1H), 7.47 (d, *J* = 2.2 Hz, 1H), 7.23 (dd, *J* = 2.4, 8.6 Hz, 1H), 7.21-7.10 (m, 3H), 7.06 (d, *J* = 8.5 Hz, 1H), 2.34 (s, 3H), 1.34 (s, 9H). Spectra were consistent with previous reports.[57]

3-*tert*-Butyl-10-acetylphenoxazine. Same general procedure using N-(2-(5-(*tert*-butyl)-2-iodophenoxy)phenyl)acetamide (2.63 g, 6.4 mmol) for the CuI catalyzed intramolecular Ullmann coupling. The product (1.26 g, 70%) was recrystallized from hexanes to render 3-*tert*-butyl-10-acetylphenoxazine as white needles; mp 139-140 °C; ^{1}H NMR (400 MHz; $CDCl_3$): δ 7.50-7.47 (m, 1H), 7.42-7.39 (m, 1H), 7.22-7.11 (m, 5H), 2.34 (s, 3H), 1.33 (s, 9H). ^{13}C NMR (101 MHz; $CDCl_3$): δ 169.3, 151.1, 150.7, 150.6, 129.6, 126.8, 125.1, 124.4, 123.2, 120.3, 116.9, 114.0, 34.7, 31.2, 23.0. HRMS (EI, magnetic sector) m/z: M+ Calcd for $C_{18}H_{19}NO_2$ 281.14158, found 281.14291.

2-Trifluoromethyl-10-acetylphenoxazine. Same general procedure using N-(2-(2-bromophenoxy)-5-(trifluoromethyl)phenyl)acetamide (3.18 g, 8.5 mmol) for the CuI catalyzed intramolecular Ullmann coupling. The crude product was purified by column chromatography (3:1, hexanes:EtOAc) to render 2-trifluoromethyl-10-acetylphenoxazine as an off-white solid (2.12 g, 85%). ^{1}H NMR (400 MHz; $CDCl_3$): δ 7.87 (d, *J* = 1.8 Hz, 1H), 7.48-7.46 (m, 1H), 7.42-7.39 (s, 1H), 7.26-7.15 (m, 4H), 2.35 (s, 3H). Spectra were consistent with previous reports.[57]

O-acetyl-3-hydroxy-10-acetylphenoxazine. Phenoxazone (0.80 g, 4.1 mmol) and anhydrous $SnCl_2$ (2.40 g, 12.7 mmol) were suspended in acetic anhydride (10 mL) with triethylamine (110 μL, 0.2 eq.). The reaction was heated to 120 °C under vigorous stirring and reaction progress monitored by TLC. After completion, the reaction was quenched in saturated Na_2CO_3 and the aqueous mixture extracted thrice with EtOAc. The organic phase was washed twice with water, dried over $MgSO_4$, filtered and the solvent removed under reduced pressure. This afforded the crude product as a light yellow solid (0.64 g, 56%) which was further purified by column chromatography (9:1, hexanes:EtOAc). ^{1}H NMR (400 MHz; benzene-d_6): δ 7.26-7.21 (m, 2H), 6.93 (d, *J* = 2.6 Hz, 1H), 6.89-6.87 (m, 1H), 6.79-6.72 (m, 2H), 6.69 (dd, *J* = 2.6, 8.7 Hz, 1H), 1.75 (s, 3H), 1.68 (s, 3H). ^{13}C NMR (101 MHz; benzene-d_6): δ 168.6, 168.5, 152.0, 151.4, 149.7, 130.4, 128.0, 127.1, 126.1, 125.9, 124.0, 117.3, 117.0, 111.2, 22.8, 20.7. HRMS (EI, magnetic sector) m/z: M+ Calcd for $C_{16}H_{13}NO_4$ 283.08446, found 283.08662.

3-Methoxy-10-acetylphenoxazine. O-acetyl-3-hydroxy-10-acetylphenoxazine (0.59 g, 2.1 mmol) was dissolved in methanol (20 mL) under a N_2 atmosphere. Stirring at room temperature, 4 mL of aqueous 10% K_2CO_3 solution was added. The reaction was monitored by TLC, with the starting material (1:1 Hexane:EtOAc, Rf = 0.50) giving way to the hydrolyzed intermediate (Rf = 0.40). The reaction mixture was quenched with 1 M HCl and extracted thrice with EtOAc. The organic phase was dried over $MgSO_4$, filtered and the solvent removed under reduced pressure. The green residue was immediately dissolved into DMF (15 mL) to which K_2CO_3 was added (0.75 g, 5.4 mmol) and the mixture was placed under a N_2 atmosphere. Under vigorous stirring, methyl iodide was added (170 μL, 2.7 mmol) and the reaction left to stir overnight. On completion, the reaction mixture was poured into water, and the aqueous mixture extracted thrice with EtOAc. The organic phase was washed twice with water, dried over $MgSO_4$, filtered and the solvent removed under reduced pressure. The residue was purified by column chromatography (3:1, hexanes:EtOAc) to render 3-methoxy-10-acetylphenoxazine as an amber coloured transparent residue (0.38 g, 71%). ^{1}H NMR (400 MHz; benzene-d_6): δ 7.37 (br, 1H), 7.20 (br, 1H), 6.98-6.96 (m, 1H), 6.83-6.76 (m, 2H), 6.63 (d, J = 2.7 Hz, 1H), 6.44 (dd, J = 2.8, 8.8 Hz, 1H), 3.18 (s, 3H), 1.83 (s, 3H). ^{13}C NMR (101 MHz; benzene-d_6): δ 168.8, 159.1, 152.6, 151.6, 130.9, 127.0, 126.3, 126.0, 123.8, 123.5, 117.2, 109.7, 102.9, 55.4, 22.8. HRMS (EI, magnetic sector) m/z: M+ Calcd for $C_{15}H_{13}NO_3$ 255.08954, found 255.09214.

3,7-Dimethoxy-10-acetylphenoxazine. 3,7-Dihydroxy-10-acetylphenoxazine (0.69 g, 2.7 mmol) and methyl iodide (340 μL, 5.5 mmol) were dissolved in DMF (15 mL) to which K_2CO_3 was added (0.79 g, 5.7 mmol). The mixture was stirred overnight at room temperature, then poured into water and the aqueous mixture extracted thrice with EtOAc. The organic phase was washed twice with water, dried over $MgSO_4$, filtered and the solvent removed under reduced pressure. An orange residue was afforded which solidified overnight on standing in a freezer. The solid was recyrstallized twice from ethanol to afford orange needles (0.42 g, 55%); mp 118-120 °C; ^{1}H NMR (400 MHz; $CDCl_3$): δ 7.38-7.36 (m, 2H), 6.70-6.67 (m, 4H), 3.81 (s, 6H), 2.29 (s, 3H). ^{13}C NMR (101 MHz; $CDCl_3$): δ 169.6, 158.3, 151.7, 125.5, 122.6, 109.0, 102.5, 55.7, 22.8. HRMS (EI, magnetic sector) m/z: M+ Calcd for $C_{16}H_{15}NO_4$ 285.10011, found 285.09708.

3-Nitro-10-acetylphenoxazine. In glacial acetic acid (12 mL) was suspended 10-acetylphenoxazine (1.12 g, 5.0 mmol) and solution of HNO_3 diluted in acetic acid (3:4,

HNO_3:AcOH, 1.4 mL) was added with swirling for ~3 minutes where the suspension dissolves to give a single red phase. The reaction mixture is allowed to stand (without stirring) for ~15 minutes after which the reaction was poured into 50 mL of water. The resulting precipitate was filtered and recrystallized from ethanol to afford the 3-nitro-10-acetylphenoxazine as orange needles (1.11 g, 82%); mp 136-138 °C; ^{1}H NMR (400 MHz; DMSO-d_6): δ 8.08 (dd, *J* = 2.7, 8.9 Hz, 1H), 8.00 (d, *J* = 2.6 Hz, 1H), 7.89 (d, *J* = 8.9 Hz, 1H), 7.65 (dd, J = 1.9, 7.9 Hz, 1H), 7.36-7.23 (m, 3H), 2.32 (s, 3H). ^{13}C NMR (101 MHz; DMSO-d_6): δ 168.9, 150.2, 149.4, 145.3, 135.2, 128.3, 127.6, 125.9, 125.2, 124.4, 119.0, 116.8, 111.9, 22.9. HRMS (EI, magnetic sector) m/z: M+ Calcd for $C_{14}H_{10}N_2O_4$ 270.06406, found 270.06128.

2-(2,4-Dinitrophenyl)amino-5-methoxyphenol. 2-Amino-5-methoxyphenol (0.32 g, 2.3 mmol) and 1-chloro-2,4-dinitrobenzene (0.47 g, 2.3 mmol) were dissolved in a mixture of ethanol (25 mL) and water (5 mL) to which sodium acetate (0.76 g, 9.3 mmol) was added. The solution was heated to reflux, under vigorous stirring for 4 hours, then allowed to cool. The reddish precipitate was filtered and purified by column chromatography (3:1, hexanes:EtOAc) to afford the product as red needles (0.59 g, 84% yield); mp 168-170 °C; ^{1}H NMR (400 MHz; DMSO-d_6): δ 9.96 (br, 1H), 9.81 (br, 1H), 8.89 (d, *J* = 2.7 Hz, 1H), 8.21 (dd, *J* = 2.7, 9.6 Hz, 1H), 7.17 (d, *J* = 8.6 Hz, 1H), 6.78 (d, *J* = 9.6 Hz, 1H), 6.57 (d, *J* = 2.7 Hz, 1H) 6.52 (dd, *J* = 2.7, 8.6 Hz, 1H), 3.75 (s, 3H). ^{13}C NMR (101 MHz; DMSO-d_6): δ 159.5, 153.5, 147.7, 135.7, 130.4, 129.6, 128.7, 123.3, 117.1, 117.0, 105.3, 102.2, 55.2. HRMS (EI, magnetic sector) m/z: M+ Calcd for $C_{13}H_{11}N_3O_6$ 305.06479, found 305.06249.

3-Methoxy-7-nitrophenoxazine (13). 2-(2,4-Dinitrophenyl)amino-5-methoxyphenol (0.22 g, 0.7 mmol) was dissolved in dry DMF (4 mL) and heated to 100 °C with stirring under a N_2 atmosphere. At 100 °C, crushed NaOH was added (70 mg, 1.75 mmol) and the mixture was heated to 120 °C for 2 hours. The reaction mixture was poured into water and extracted 3 times with Et_2O. The organic solution was washed twice with water, dried over $MgSO_4$, filtered and the solvent removed under reduced pressure. The product was purified by column chromatography (3:1, hexanes:EtOAc) to afford a deep red solid (0.10 g, 55%) ^{1}H NMR (400 MHz; DMSO-d_6): δ 9.27 (br, 1H), 7.69 (dd, *J* = 2.6, 8.8 Hz, 1H), 7.31 (d, *J* = 2.6 Hz), 6.48 (d, *J* = 8.5 Hz, 1H), 6.47 (d, *J* = 8.8 Hz, 1H), 6.40 (dd, *J* = 2.7, 8.5 Hz, 1H), 6.36 (d, *J* = 2.7 Hz, 1H), 3.65 (s, 3H). ^{13}C NMR (75 MHz; DMSO-d_6): δ 155.3, 142.8, 141.4, 139.9, 138.8, 122.5, 122.2, 114.6, 111.6, 110.0, 108.7,

102.5, 55.4. HRMS (EI, magnetic sector) m/z: M+ Calcd for $C_{13}H_{10}N_2O_4$ 258.06406, found 258.06296.

N,N-Diethyl-3-sulfonamidephenoxazine (11). 3,4-Difluorobenzenesulfonyl chloride (0.81 g, 3.8 mmol) was dissolved into dry DCM (4.3 mL) cooled to 0 °C. Under vigorous stirring, diethylamine was added (1.4 mL, 3 eq.). Once the difluorobenzenesulfonyl chloride was consumed, the mixture was poured into water and extracted twice with EtOAc. The organic solution was dried over $MgSO_4$, filtered and the solvent removed under reduced pressure. The resulting solid was dissolved in DMSO (20 mL) and placed in a sealed tube along with 2-aminophenol (0.42 g, 3.8 mmol) to which K_2CO_3 was added (1.33 g, 9.6 mmol). The reaction was heated to 135 °C for 14 hours with vigorous stirring after which the reaction was cooled, quenched with water and the aqueous mixture extracted thrice with EtOAc. The organic phase was washed twice with water, dried over $MgSO_4$, filtered and the solvent removed under reduced pressure. The crude solid was purified by column chromatography (3:1, hexanes:EtOAc) to render the product as off-white solid (0.85 g, 70%) and subsequently recrystallized from Et_2O to afford off-white needles; mp 154-156 °C; ^{1}H NMR (400 MHz; DMSO-d_6): δ 8.81 (b, 1H), 7.14 (dd, *J* = 2.1, 8.2 Hz, 1H), 6.84 (d, *J* = 2.1 Hz, 1H), 6.77-6.74 (m, 1H), 6.66-6.61 (m, 2H), 6.52 (d, *J* = 8.2 Hz, 1H), 6.49-6.47 (m, 1H), 3.10 (q, *J* = 7.2 Hz, 4H), 1.04 (t, *J* = 7.2 Hz, 6H). ^{13}C NMR (101 MHz; DMSO-d_6): δ 142.6, 142.4, 136.6, 130.7, 130.2, 124.4, 123.9, 121.5, 115.2, 113.2, 113.1, 112.7, 41.7, 14.1. HRMS (EI, magnetic sector) m/z: M+ Calcd for $C_{16}H_{18}N_2O_3S$ 318.10381, found 318.10173.

2,4,6,8-Tetra-*tert*-butylphenoxazine (9). To a solution of 2,4-di-*tert*-butyl-6-nitrophenol (5.5 g, 0.022 mol) in glacial acetic acid (88 mL) was added zinc dust (5.0 g, 0.077 mol) in portions with vigorous stirring while heating to 90 °C. The slurry was held at 90 °C for 45 minutes and refluxed for 15 minutes. After cooling the mixture was poured into water and extracted thrice with Et_2O. The organic phase was washed with water, dried over $MgSO_4$, filtered and the solvent removed under reduced pressure. The residue was purified by column chromatography (95:5, pet. ether:Et_2O) to render a light purple solid which was recyrstallized from hexanes to afford 2,4,6,8-tetra-*tert*-butylphenoxazine (0.76 g, 17%); mp 191-193 °C; ^{1}H NMR (400 MHz; DMSO-d_6): δ 7.83 (br, 1H), 6.53 (s, 2H), 6.29 (s, 2H), 1.38 (s, 18H), 1.18 (s, 18H). ^{13}C NMR (101 MHz; DMSO-d_6): δ 144.8, 139.3, 135.1, 132.0, 114.4, 108.8, 34.2, 33.8, 31.0, 30.5. HRMS (EI, magnetic sector) m/z: M+ Calcd for $C_{28}H_{41}NO$ 407.31881, found 407.31979.

2,8-Di-*tert*-butylphenoxazine (10). To a solution of 2,4-di-*tert*-butyl-6-nitrophenol (5.5 g, 0.022 mol) in glacial acetic acid (88 mL) was added zinc dust (5.0 g, 0.077 mol) by portion with vigorous stirring while heating to 90 °C. The slurry was held at 90 °C for 45 minutes and refluxed for 30 minutes. After cooling the mixture was poured into water and extracted thrice with EtOAc. The organic phase was washed with water, dried over $MgSO_4$, filtered and the solvent removed under reduced pressure. The residue was purified by column chromatography (95:5,hexane:EtOAc) to render a dark violet oil. It was dissolved in glacial acetic acid and zinc was added until the solution was colorless, which was then quenched with Na_2CO_3 solution and extracted with EtOAc. After removal of the solvent, a violet solid was afforded which was recrystallized from hexanes to afford the 2,8-di-*tert*-butylphenoxazine (0.24 g, 7%) as purple needles; mp 161-162 °C; ^{1}H NMR (400 MHz; benzene-d_6): δ 6.71 (d, J = 8.3 Hz, 2H), 6.54 (dd, J = 2.3, 8.3 Hz, 2H), 6.11 (d, J = 2.3 Hz, 2H), 4.07 (b, 1H), 1.24 (s, 18H). ^{13}C NMR (101 MHz; DMSO-d_6): δ 146.1, 140.7, 131.8, 116.6, 114.4, 110.4, 33.8, 31.1. HRMS (EI, magnetic sector) m/z: M+ Calcd for $C_{20}H_{25}NO$ 295.19361, found 295.19103.

3-Nitro-7-cyanophenoxazine (15). 3-Cyanophenoxazine (0.50 g, 2.4 mmol) was suspended in glacial acetic acid (25 mL) and acetonitrile was added until the solute dissolved (6 mL). With stirring, 1.1 eq. of 70% HNO_3 was added, immediately the product crashed out as an orange amorphous precipitate (0.39 g, 65%) which was filtered and rinsed with Et_2O. The product was further purified by column chromatography (1:1, hexanes:EtOAc) and recrystallized from ethanol to afford fine red needles; 215-220 °C (decomposes); ^{1}H NMR (400 MHz; DMSO-d_6): δ 9.83 (s, 1H), 7.71 (dd, J = 2.6, 8.7 Hz, 1H), 7.34 (d, J = 2.5 Hz, 1H), 7.24 (dd, J = 1.8, 8.1 Hz, 1H), 7.07 (d, J = 1.7 Hz, 1H), 6.58 (d, J = 8.1 Hz, 1H), 6.56 (d, J = 8.7 Hz, 1H). ^{13}C NMR (101 MHz; DMSO-d_6): δ 142.3, 142.1, 140.7, 137.8, 134.8, 130.1, 121.9, 118.6, 118.1, 114.4, 113.0, 110.2, 103.4. HRMS (EI, magnetic sector) m/z: M+ Calcd for $C_{13}H_7N_3O_3$ 253.04874, found 253.05072.

3-Trifluoromethylphenoxazine (5). In sealed tube flushed with N_2 were added 1-iodo-2-(2-nitrophenoxy)-4-(trifluoromethyl)benzene (0.97 g, 2.3 mmol), K_2CO_3 (0.64 g, 4.6 mmol), copper(I) iodide (24 mg, 0.05 eq.), N,N'-dimethylethylenediamine (25 μL, 0.10 eq.), and toluene (10 mL). The reaction was heated to 130 °C under vigorous stirring for at least 10 hours. After completion, the reaction mixture was diluted with dichloromethane and passed through a plug of silica, after which the solvent was removed under reduced pressure. The residue was dissolved in

EtOH (20 mL) with stirring and was placed under N_2 and heated to 75 °C to which 33% aqueous HCl was added (5 mL). The reaction was monitored by TLC, and after 2 hours the mixture was cooled then quenched with Na_2CO_3 solution. The aqueous mixture was extracted 3 times with EtOAc. The organic solution was washed twice with water, dried over $MgSO_4$, filtered and the solvent removed under reduced pressure. The crude product was recrystallized from hexanes to afford beige plates (0.36 g, 61%); mp 145-146 °C; ^{1}H NMR (400 MHz; DMSO-d_6): δ 8.70 (br, 1H), 7.07-7.04 (m, 1H), 6.85 (d, J = 2.0 Hz, 1H), 6.79-6.73 (m, 1H), 6.65-6.61 (m, 2H) 6.54 (dd, 0.7, 8.2 Hz, 1H), 6.49-6.47 (m, 1H). ^{13}C NMR (101 MHz; DMSO-d_6): δ 142.8, 142.4, 136.3, 131.0, 124.4, 124.1 (q, $J_{C\text{-}F}$ = 270.7 Hz), 121.5 (q, $J_{C\text{-}F}$ = 4.4 Hz), 121.4, 120.2 (q, $J_{C\text{-}F}$ = 32.6 Hz), 115.2, 113.7, 112.9, 111.7 (q, $J_{C\text{-}F}$ = 3.7 Hz). ^{19}F NMR (376 MHz, $CDCl_3$): δ -63.41. HRMS (EI, magnetic sector) m/z: M+ Calcd for $C_{13}H_8F_3NO$ 251.05580, found 251.05612.

3,7-Di-*tert*-butylphenoxazine (8). Same general procedure using N-(4-(*tert*-butyl)-2-(5-(*tert*-butyl)-2-iodophenoxy)phenyl)acetamide (0.68 g, 1.5 mmol) for the CuI catalyzed intramolecular Ullmann coupling followed by subsequent amide hydrolysis in EtOH. The product was recrystallized from hexanes to afford white needles (0.18 g, 41%); mp 185-187 °C; ^{1}H NMR (400 MHz; DMSO-d_6): δ 7.96 (br, 1H), 6.72 (dd, J = 2.2, 8.1 Hz, 2H), 6.61 (d, J = 2.1 Hz, 2H), 6.36 (d, J = 8.1 Hz, 2H), 1.18 (s, 18H). ^{13}C NMR (101 MHz; DMSO-d_6): δ 142.9, 142.3, 130.0, 119.9, 112.6, 112.3, 33.7, 31.1. HRMS (EI, magnetic sector) m/z: M+ Calcd for $C_{20}H_{25}NO$ 295.19361, found 295.19103.

2-*tert*-Butylphenoxazine (6). 10-Acetyl-2-*tert*-butylphenoxazine (237 mg, 0.84 mmol) was dissolved in EtOH (5 mL) with stirring and was placed under N_2 and heated to 75 °C to which 33% aqueous HCl was added (1 mL). The reaction was monitored by TLC, and after 2 hours the mixture was cooled then quenched with Na_2CO_3 solution. The aqueous mixture was extracted 3 times with EtOAc. The organic phase was washed twice with water, dried over $MgSO_4$, filtered and the solvent removed under reduced pressure. The crude product was recrystallized from hexanes to afford silver plates (130 mg, 65%); mp 125-127 °C; ^{1}H NMR (400 MHz; DMSO-d_6): δ 8.10 (br, 1H), 6.70 (ddd, J = 1.8, 7.6, 7.6 Hz, 1H), 6.59-6.51 (m, 4H), 6.47 (d, J = 2.2 Hz, 1H), 6.43 (dd, J = 1.4, 7.6 Hz, 1H), 1.19 (s, 9H). ^{13}C NMR (101 MHz; DMSO-d_6): δ 146.3, 142.8, 140.5, 132.5, 131.7, 123.7, 120.1, 116.8, 115.0, 114.4, 113.2, 110.5, 33.8, 31.1. HRMS (EI, magnetic sector) m/z: M+ Calcd for $C_{16}H_{17}NO$ 239.13101, found 239.12987.

3-*tert*-Butylphenoxazine (7). Same general amide hydrolysis with 10-acetyl-3-tert-butylphenoxazine (155 mg, 0.55 mmol). The product was recrystallized from hexanes to afford fine white needles (90 mg, 68%); mp 132-135 °C; ^{1}H NMR (400 MHz; DMSO-d_6): δ 8.06 (br, 1H), 6.73-6.68 (m, 2H), 6.62 (d, J = 2.1 Hz, 1H), 6.59-6.52 (m, 2H), 6.43 (dd, J = 1.5, 7.7 Hz, 1H), 6.37 (d, J = 8.1 Hz, 1H), 1.18 (s, 9H). ^{13}C NMR (101 MHz; DMSO-d_6): δ 143.2, 142.7, 142.3, 132.6, 129.7, 123.8, 120.02, 120.00, 115.0, 113.2, 112.7, 112.3, 33.7, 31.1. HRMS (EI, magnetic sector) m/z: M+ Calcd for $C_{16}H_{17}NO$ 239.13101, found 239.12987.

2-Trifluoromethylphenoxazine (4). Same general amide hydrolysis with 10-acetyl-2-trifluoromethylphenoxazine (2.17 g, 7.4 mmol). The product was resolved as white prismatic crystals (1.48 g, 80%); mp 153-154 °C; ^{1}H NMR (400 MHz; DMSO-d_6): δ 8.51 (br, 1H), 6.90-6.87 (m, 1H), 6.79-6.73 (m, 2H), 6.66-6.59 (m, 3H), 6.46 (dd, J = 1.4, 7.6 Hz, 1H). ^{13}C NMR (101 MHz; DMSO-d_6): δ 145.8, 142.2, 133.3, 131.2, 124.60 (q, $J_{C\text{-}F}$ = 32.3 Hz), 124.55, 124.0 (q, $J_{C\text{-}F}$ = 271.4 Hz), 121.1, 117.5 (q, $J_{C\text{-}F}$ = 4.4 Hz), 115.4, 115.3, 113.6, 109.2 (q, $J_{C\text{-}F}$ = 3.7 Hz) ^{19}F NMR (376 MHz, $CDCl_3$): δ -63.78. HRMS (EI, magnetic sector) m/z: M+ Calcd for $C_{13}H_8F_3NO$ 251.05580, found 251.05441.

3-Nitrophenoxazine (14). Same general amide hydrolysis with 10-acetyl-3-nitrophenoxazine (300 mg, 1.1 mmol). After quenching with Na_2CO_3 solution the product precipitated out and was then filtered and washed with a minimum of methanol followed by petroleum ether to afford fine olive coloured needles (230 mg, 91%); mp 185-188 °C; ^{1}H NMR (400 MHz; DMSO-d_6): δ 9.34 (br, 1H), 7.67 (dd, J = 2.4, 8.7 Hz, 1H), 7.31 (d, J = 2.4 Hz, 1H), 6.81-6.77 (m, 1H), 6.71-6.64 (m, 2H), 6.53-6.48 (m, 2H). ^{13}C NMR (101 MHz; DMSO-d_6): δ 142.20, 142.18, 139.7, 139.5, 129.5, 124.5, 122.6, 121.9, 115.3, 114.3, 111.9, 110.0. HRMS (EI, magnetic sector) m/z: M+ Calcd for $C_{12}H_8N_2O_3$ 228.05349, found 228.05201.

3-Methoxyphenoxazine (16). Same general amide hydrolysis with 10-acetyl-3-methoxyphenoxazine (380 mg, 1.5 mmol). The charcoal coloured solid afforded required no further purification. ^{1}H NMR (400 MHz; DMSO-d_6): δ 7.93 (br, 1H), 6.72 (ddd, J = 1.6, 7.6, 7.6 Hz, 1H), 6.60-6.51 (m, 2H), 6.43 (dd, J = 1.5, 7.7 Hz, 1H), 6.40-6.29 (m, 3H), 3.63 (s, 3H). ^{13}C NMR (101 MHz; DMSO-d_6): δ 153.7, 143.2, 142.1, 132.8, 125.6, 124.0, 119.7, 115.0, 113.4, 113.1, 108.1, 102.4, 55.3. HRMS (EI, magnetic sector) m/z: M+ Calcd for $C_{13}H_{11}NO_2$ 213.07898, found 213.07801.

3,7-Dimethoxyphenoxazine (17). Same general amide hydrolysis with 10-acetyl-3,7-dimethoxyphenoxazine (395 mg, 1.4 mmol). After quenching with Na_2CO_3 solution the product began to precipitate as needles. The flask was placed in the freezer overnight and the product was filtered the following day to afford the maroon coloured product (257 mg, 75%). ^{1}H NMR (400 MHz; DMSO-d_6): δ 7.68 (br, 1H), 6.39-6.30 (m, 6H), 3.63 (s, 6H). ^{13}C NMR (101 MHz; DMSO-d_6): δ 155.3, 142.5, 126.1, 113.4, 108.3, 102.4, 55.3. HRMS (EI, magnetic sector) m/z: M+ Calcd for $C_{14}H_{13}NO_3$ 243.08954, found 243.09118.

Inhibited Co-autoxidation of PBD-BODIPY and Styrene. To a 3 mL cuvette was added 1.25 mL of purified styrene and 1.18 mL of PhCl. The cuvette was placed in the sample holder of a UV-visible spectrophotometer and equilibrated to 37 °C. PBD-BODIPY (12.5 μL of a 2.0 mM solution in 1,2,4-trichlorobenzene) was added, succeeded by 50 μL of 0.3 M AIBN in PhCl, and the contents of cuvette briefly agitated to thoroughly mix the contents. The absorbance at 591 nm was monitored for 15 minutes to ensure linear reaction progress, after which 10 μL of a 0.5 mM solution of inhibitor was added followed by thorough mixing for a final antioxidant concentration of 2 μM (unless noted otherwise). The rate of initiation (R_i = 2.7 × 10^{-9} M s^{-1}) was determined using PMC as a standard, which has an established stoichiometry of n = 2.[61]

Inhibited Co-autoxidation of PBD-BODIPY and Dioxane. To a 3 mL cuvette was added 620 μL of certified ACS 1,4-dioxane and either 1.80 mL of PhCl or 1.18 mL of PhCl with 620 μL of DMSO. The following steps are identical to the protocol described immediately above) though the absorbance was monitored at 587 nm (ε = 123 000 M^{-1} cm^{-1} in PhCl, ε = 118 200 M^{-1} cm^{-1} in 2:1 PhCl:DMSO). The rate of initiation in PhCl (R_i = 2.4 × 10^{-9} M s^{-1}) and in 2:1 PhCl:DMSO (R_i = 2.1 × 10^{-9} M s^{-1}) required to determine stoichiometric data were standardized by PMC and tetrahydronaphthyridinol (C_{10}-THN, structure in ESI)[62] respectively maintaining that n = 2. The rate constant for propagation by PBD-BODIPY in the aforementioned solvent systems ($k_{\text{PBD-BODIPY}}$ = 5310 M^{-1} s^{-1} and $k_{\text{PBD-BODIPY}}$ = 5900 M^{-1} s^{-1}) were determined from the uninhibited rate of PBD-BODIPY consumption under the conditions of the experiment assuming that k_t is equal to that of the peroxyl derived from 1,4-dioxane (k_t = 2.5 × 10^7 M^{-1} s^{-1})[19] and calculated from the previously derived Eq. 8:[14]

$$\frac{-\delta[\text{PBD}-\text{BODIPY}]}{\delta t} = \frac{k_{\text{PBD}-\text{BODIPY}}}{\sqrt{2k_t}}\sqrt{R_i}[\text{PBD}-\text{BODIPY}] \qquad (8)$$

R_i and $k_{PBD\text{-}BODIPY}$ provide the means to calculate k_{inh}^{Diox} and k_{inh}^{DMSO} with Eq. 3 in Figure 1C.

Determination of Solvent Mixture β_2^H by ^{19}F NMR. The H-bond accepting solvent mixture of interest was diluted into CCl_4 to render four dilute solutions of varying concentrations (see ESI) and one 1.2 M solution. To these were added 4-fluorophenol and 4-fluoroanisole to a final concentration of 0.01 M of each. The solutions were transferred into NMR tubes containing sealed capillaries of benzene-d_6 with α,α,α-trifluorotoluene, after which their ^{19}F NMR spectra were obtained at multiple temperatures using a thermostatted 300 MHz NMR instrument. At a given temperature, the K_f of the 4-fluorophenol and the H-bond acceptor(s) is described by Eq. 9:[22]

$$K_f = \frac{(\delta/\Delta)A_0}{\{A_0[1-(\delta/\Delta)]\}[B_0-(\delta/\Delta)A_0]} \quad (9)$$

where A_0 is the concentration of 4-fluorophenol, B_0 is the concentration of H-bond acceptor(s), Δ is the chemical shift difference between 4-fluorophenol and 4-fluoroanisole at B_0 = 1.20 M and δ is the chemical shift difference between 4-fluorophenol and 4-fluoroanisole at the dilute concentrations of H-bond acceptor(s). The effective β_2^H can be calculated from this K_f via Eq. 10 and Eq. 11:

$$\log K_f = L_A \log K_B^H + D_A \quad (10)$$

$$\beta_2^H = (\log K_B^H + 1.1)/\,4.636 \quad (11)$$

where L_A = 1 and D_A = 0 when the reference H-bond donor is 4-fluorophenol.[18]

Determination of Phenoxazine α_2^H by ^{1}H NMR. Two ~3 mg portions of the H-bond donor species of interest were dissolved into 700 μL of each of DMSO-d_6 and benzene-d_6. The ^{1}H NMR spectra of each were obtained and the chemical shifts were referenced to the residual solvent peaks of the solvents (2.50 ppm and 7.16 ppm for DMSO and benzene, respectively.) The α_2^H value was then determined from the difference in the chemical shift of the proton of interest between the two spectra ($\Delta\delta_{DMSO\text{-}Ben}$) as in Eq. 7:

$$\alpha_2^H = 0.134\Delta\delta_{DMSO-Ben} - 0.1087 \quad (7)$$

The correlation of α_2^H and $\Delta\delta_{DMSO\text{-}Ben}$ was constructed by obtaining ^{1}H NMR spectra in both DMSO-d_6 and benzene-d_6 for 11 different H-bond donors whose α_2^H values (ranging from 0.08 to

0.82) were independently determined and plotting the chemical shift differences ($\Delta\delta_{DMSO\text{-}Ben}$) vs. α_2^H. See ESI for further elaboration.

Electrochemistry. Standard potentials were measured by cyclic voltammetry at 25 °C in dry acetonitrile containing $Bu_4N^+PF_6^-$ (0.1 M) as electrolyte. Experiments were carried out with a potentiostat equipped with a glassy-carbon working electrode, a platinum auxiliary electrode, and a $Ag/AgNO_3$ (0.005 M) reference electrode. The given E^o were determined relative to the ferrocene/ferrocenium couple under the same conditions (Fc/Fc^+ vs NHE +0.64 V).[63]

Computations. Quantum chemical calculations were carried out using the CBS-QB3 complete basis set method[64] as it is implemented in the Gaussian 09 suite of programs.[65] Molecular orbitals were rendered at an isovalue of 0.015 using the B3LYP/CBSB7 wavefunctions.

Acknowledgements. This work was supported by grants from the Natural Sciences and Engineering Research Council of Canada and the Canada Foundation for Innovation. DAP and EAH also acknowledge the support of the Canada Research Chairs and Ontario Graduate Scholarships programs, respectively.

Associated Content.

Supporting Information

The supporting information is available free of charge on the ACS Publications website at DOI:

Standardization of co-autoxidations, β_2^H and α_2^H parameter determination, co-autoxidation data, cyclic voltammograms, NMR spectra, and computational data.

References.

(1) Ingold, K. U. *Chem. Rev.* **1961**, *61*, 563–589.

(2) Ingold, K. U.; Pratt, D. A. *Chem. Rev.* **2014**, *114*, 9022–9046.

(3) Pratt, D. A.; DiLabio, G. A.; Mulder, P.; Ingold, K. U. *Acc. Chem. Res.* **2004**, *37*, 334–340.

(4) Valgimigli, L.; Pratt, D. A. In *Encyclopedia of Radicals in Chemistry, Biology and*

Materials; John Wiley & Sons, Ltd: Chichester, UK, 2012; pp 1623–1677.

(5) (a) Brownlie, I. T.; Ingold, K. U. *Can. J. Chem.* **1967**, *45*, 2419–2425; (b) Hansch, C.; Gao, H. *Chem. Rev.*, **1997**, *97*, 2995-3059.

(6) Lucarini, M.; Pedrielli, P.; Pedulli, G. F.; Valgimigli, L.; Gigmes, D.; Tordo, P. *J. Am. Chem. Soc.* **1999**, *121*, 11546–11553.

(7) Pratt, D. A.; Dilabio, G. A.; Valgimigli, L.; Pedulli, G. F.; Ingold, K. U. *J. Am. Chem. Soc.* **2002**, *124*, 11085–11092.

(8) (a) Hanthorn, J. J.; Valgimigli, L.; Pratt, D. A. *J. Am. Chem. Soc.* **2012**, *134*, 8306–8309; (b) Hanthorn, J. J.; Valgimigli, L.; Pratt, D. A. *J. Org. Chem.* **2012**, *77*, 6895-6907.

(9) The value reported in reference 6 should be reduced by 1.1 kcal mol^{-1} to account for the revised O–H BDE of 2,4,6-tri-*tert*-butylphenol used as the reference in the radical equilibration EPR measurements. See: Mulder, P.; Korth, H.-G.; Pratt, D. A.; Dilabio, G. A.; Valgimigli, L.; Pedulli, G. F.; Ingold, K. U. *J. Phys. Chem. A* **2005**, *109*, 2647–2655.

(10) In previous work we have shown that some substituted heteroaryl (i.e. pyridyl and pyrimidyl) analogues of diphenylamines are similarly reactive, with k_{inh} values up to ~4 × 10^7 M^{-1} s^{-1}. See references 8a and 8b.

(11) The half-wave potentials of phenothiazine (0.82 V [6] and 0.83 V,[a] $E^{1/2}$ vs. NHE) and phenoxazine (0.83 V,[b] $E^{1/2}$ vs. NHE) have been reported (measured in acetonitrile with a saturated calomel electrode). Using an identical potentiostat, condition and internal standard (see Experimental VII) we consistently measured E^o ($E^{1/2}$ vs. NHE) of 0.85 and 0.87 V for phenothiazine and phenoxazine, respectively. See: (a) Billon, J.-P. *Ann. Chim.*, **1962**, *7*, 183. (b) Kowert, B. A.; Marcoux, L.; Bard, A. J. *J. Am. Chem. Soc.*, **1972**, *94*, 5538–5550.

(12) Howard, J. A.; Ingold, K. U. *Can. J. Chem.* **1962**, *40*, 1851–1864.

(13) Burton, G. W.; Ingold, K. U. *J. Am. Chem. Soc.* **1981**, *103*, 6472–6477.

(14) Haidasz, E. A.; Van Kessel, A. T. M.; Pratt, D. A. *J. Org. Chem.* **2016**, *81*, 737–744.

(15) Snelgrove, D. W.; Lusztyk, J.; Banks, J. T.; Mulder, P.; Ingold, K. U. *J. Am. Chem. Soc.*

2001, *123*, 469–477.

(16) Litwinienko, G.; Ingold, K. U. *Acc. Chem. Res.* **2007**, *40*, 222–230.

(17) Abraham, M. H.; Grellier, P. L.; Prior, D. V.; Duce, P. P.; Morris, J. J.; Taylor, P. J. *J. Chem. Soc. Perkin Trans. 2* **1989**, 699–711.

(18) Abraham, M. H.; Grellier, P. L.; Prior, D. V.; Morris, J. J.; Taylor, P. J. *J. Chem. Soc. Perkin Trans. 2* **1990**, 521–529.

(19) Howard, J. A.; Ingold, K. U. *Can. J. Chem.* **1969**, *47*, 3809–3815.

(20) Arnett, E. M.; Joris, L.; Mitchell, E.; Murty, T. S. S. R.; Gorrie, T. M.; Schleyer, P. von R. *J. Am. Chem. Soc.* **1970**, *92*, 2365–2377.

(21) Foti, M. C.; Barclay, L. R. C.; Ingold, K. U. *J. Am. Chem. Soc.* **2002**, *124*, 12881–12888.

(22) Taft, R. W.; Gurka, D.; Joris, L.; von Schleyer, R.; Rakshys, J. W. *J. Am. Chem. Soc.* **1969**, *91*, 4794–4801.

(23) The log K_f for complex formation between 4-fluorophenol and the HBA was determined for the temperature at which the inhibited autoxidations were carried out (37 °C). See ESI for further elaboration.

(24) Abraham, M. H.; Abraham, R. J.; Byrne, J.; Griffiths, L. *J. Org. Chem.* **2006**, *71*, 3389–3394.

(25) Chlorobenzene is the most commonly used solvent for inhibited autoxidation experiments, dating back over 50 years. Hence, we have used this as the reference medium in order to enable comparisons to previously reported data.

(26) The synthesis of 5-hydroxy-4,6-dimethyl-2-dimethylaminopyrimidine **C**[a] and 5-hydroxy-2-dimethylaminopyrimidine **B**[b] and the α_2^H of PMC **A** (0.38)[c] and compound **C** (0.53)[c] were previously reported. See: (a) Pratt, D. A.; DiLabio, G. A.; Brigati, G.; Pedulli G. F.; Valgimigli, L. *J. Am. Chem. Soc.*, **2001**, *123*, 4625–4626. (b) Nara, S. J.; Jha, M.; Brinkhorst, J.; Zemanek, T. J.; Pratt, D. A. *J. Org. Chem.*, **2008**, *73*, 9326–9333. (c) Valgimigli, L.; Bartolomei, D.; Amorati, R.; Haidasz, E.; Hanthorn, J. J.; Nara, S. J.;

Brinkhorst, J.; Pratt, D. A. *Beilstein J. Org. Chem.*, **2013**, *9*, 2781–2792.

(27) Chauvin, J.-P. R.; Griesser, M.; Pratt, D. A. *J. Am. Chem. Soc.* **2017**, *139*, 6484–6493.

(28) Burton, G. W.; Ingold, K. U. *Acc. Chem. Res.* **1986**, *19*, 194–201.

(29) Rickert, H. B.; Geiger, W. M. 2,4,6,8-Tetra-Tertiarybutylphenoxazine. US 2945856, 1960.

(30) Eastmond, G. C.; Gilchrist, T. L.; Paprotny, J.; Steiner, A. *New J. Chem.* **2001**, *25*, 385–390.

(31) Kolchina, E. F.; Kargapolova, I. Y.; Gerasimova, T. N. *Bull. Acad. Sci. USSR Div. Chem. Sci.* **1986**, *35*, 1685–1689.

(32) Moore, L. O. Reactions of phenoxazine and some of its derivatives. Ph. D. Dissertation, Iowa State College, 1957.

(33) Hansch, C.; Leo, A.; Taft, R. W. *Chem. Rev.* **1991**, *91*, 165–195.

(34) These calculations exhibit strong spin contamination presumably due to the the heavily delocalized π-system of the phenoxazine aminyl radical. Calculations carried out within the restricted open shell formalism (ROCBS-QB3) were also performed for a few representative cases. Interestingly, these calculations further underestimated the BDEs (e.g. the BDE of phenoxazine was calculated to be 73.0 and 75.2 kcal mol^{-1} by ROCBS-QB3 and CBS-QB3, respectively, which can be compared to the experimental value of 76.1 kcal mol^{-1}).

(35) It has previously been observed that the N-H BDEs in di-substituted diphenylamines and phenothiazines also correlate very well with the sum of the σ_p^+ substituent constants. See ref. 7.

(36) DiLabio, G. A.; Johnson, E. R. *J. Am. Chem. Soc.* **2007**, *129*, 6199–6203.

(37) Vaidya, V.; Ingold, K. U.; Pratt, D. A. *Angew. Chemie Int. Ed.* **2009**, *48*, 157–160.

(38) Amorati, R.; Pedulli, G. F.; Pratt, D. A.; Valgimigli, L. *Chem. Commun.* **2010**, *46*, 5139–5141.

(39) Zielinski, Z.; Presseau, N.; Amorati, R.; Valgimigli, L.; Pratt, D. A. *J. Am. Chem. Soc.* **2014**,

136, 1570–1578.

(40) Massie, S. P. *Chem. Rev.* **1954**, *54*, 797–833.

(41) The synthesis of phenoxazine has historically been accomplished by high temperature melts of catechol and o-aminophenol or o-aminophenol along with its corresponding hydrochloride salt. However, isolation and purification of the product from these routes can be arduous. Judging by more recent attempts to improve the process, it would seem a highly efficient and cost effective synthetic route has yet to be identified. See: (a) Bernthsen, A. *Chem. Ber.* **1887**, *20*, 943. (b) Kehrmann, F.; Neil, A. A. *Chem. Ber.***1914**, *47*, 3102. (c) Gaddam, O. R.; Mamillapali, R. S.; Batchu, C.; Chebiyyam, P. An Improved Process for the Preparation of 10H-Phenoxazine. WO2002034732, 2000.

(42) Murphy, C. M.; Ravner, H.; Smith, N. L. *Ind. Eng. Chem.* **1950**, *42*, 2479–2489.

(43) Warren, J. J.; Mayer, J. M. *Proc. Natl. Acad. Sci.* **2010**, *107*, 5282–5287.

(44) Bietti, M.; Salamone, M.; DiLabio, G. A.; Jockusch, S.; Turro, N. J. *J. Org. Chem.* **2012**, *77*, 1267–1272.

(45) Previously Arrhenius plots spanning 310-368 K for H-atom transfer to peroxyl radicals by diarylamines indicated log A ~ 6.9-7.1. However, examples of highly reactive diarylamines converge at log k ~ 7.5, suggesting that log A ~ 7.5 is probable – see ref. 8.

(46) Wijtmans, M.; Pratt, D. A.; Valgimigli, L.; DiLabio, G. A.; Pedulli, G. F.; Porter, N. A. *Angew. Chemie Int. Ed.* **2003**, *42*, 4370–4373.

(47) Jonsson, M.; Wayner, D. D. M.; Lusztyk, J. *J. Phys. Chem.* **1996**, *100*, 17539–17543.

(48) Jensen, R. K.; Korcek, S.; Zinbo, M.; Gerlock, J. L. *J. Org. Chem.* **1995**, *60*, 5396–5400.

(49) Haidasz, E. A.; Shah, R.; Pratt, D. A. *J. Am. Chem. Soc.* **2014**, *136*, 16643–16650.

(50) The activation energy required to regenerate the diarylamine via homolysis and in-cage disproportionation is intrinsically related to the N-O BDE. Assuming that the difference in N-H BDEs of ADPAs and phenoxazine (6.1 kcal mol^{-1}) manifests itself fully in the difference in the strength of the weaker N-O bond, E_a for a phenoxazine-derived

alkoxyamine can be estimated to be 27.4 kcal mol^{-1} (compared to ADPA where E_a = 33.5 kcal mol^{-1}),[49] which corresponds to a unimolecular rate constant on the order of 10^{-5} s^{-1} at 37°C – 10 orders of magnitude lower than that required to produce the observed secondary inhibited period (~ 10^5 M^{-1} s^{-1}).

(51) Calculated from the half wave potential from the cyclic voltammogram of α-tocopherol and adjusted to a NHE reference (Fc/Fc^+ *vs*. NHE = +0.64 V). See: Williams, L. L.; Webster, R. D. *J. Am. Chem. Soc.*, **2004**, *126*, 12441–12450.

(52) Shah, R.; Margison, K. D.; Pratt, D. A. *ACS Chem. Biol.* [Just Accepted], DOI: 10.1021/acschembio.7b00730. Published online: August 24, 2017.

(53) Moosmann, B.; Skutella, T.; Beyer, K.; Behl, C. *Biol. Chem.* **2001**, *382*, 1601–1612.

(54) Kehrmann, F.; Boubis, A. *Berichte der Dtsch. Chem. Gesellschaft* **1917**, *50*, 1662–1667.

(55) Du, C.; Zheng, C.; Fifth, Z. Hepatitis b surface antigen and antibody detection method. CN 101334407 A, 2008.

(56) Granick, S.; Michaelis, L.; Schubert, M. P. *J. Am. Chem. Soc.* **1940**, *62*, 1802–1810.

(57) Thomé, I.; Bolm, C. *Org. Lett.* **2012**, *14*, 1892–1895.

(58) Kormos, A.; Móczár, I.; Sveiczer, A.; Baranyai, P.; Párkányi, L.; Tóth, K.; Huszthy, P. *Tetrahedron* **2012**, *68*, 7063–7069.

(59) Delor, M.; Keane, T.; Scattergood, P. A.; Sazanovich, I. V.; Greetham, G. M.; Towrie, M.; Meijer, A. J. H. M.; Weinstein, J. A. *Nat. Chem.* **2015**, *7*, 689–695.

(60) Doad, G. J. S.; Barltrop, J. A.; Petty, C. M.; Owen, T. C. *Tetrahedron Lett.* **1989**, *30*, 1597–1598.

(61) Burton, G. W.; Doba, T.; Gabe, E.; Hughes, L.; Lee, F. L.; Prasad, L.; Ingold, K. U. *J. Am. Chem. Soc.* **1985**, *107*, 7053–7065.

(62) Zilka, O.; Shah, R.; Li, B.; Friedmann Angeli, J. P.; Griesser, M.; Conrad, M.; Pratt, D. A. *ACS Cent. Sci.* **2017**, *3*, 232–243.

(63) Pegis, M. L.; Roberts, J. A. S.; Wasylenko, D. J.; Mader, E. A.; Appel, A. M.; Mayer, J. M. *Inorg. Chem.* **2015**, *54*, 11883–11888.

(64) Montgomery, J. A.; Frisch, M. L.; Ochterski, J. W.; Petersson, G. A. *J. Chem. Phys.* **1999**, 110, 2822–2827.

(65) Frisch, M. J.; Trucks, G. W.; Schlegel, H. B.; Scuseria, G. E.; Robb, M. A.; Cheeseman, J. R.; Scalmani, G.; Barone, V.; Mennucci, B.; Petersson, G. A.; Nakatsuji, H.; Caricato, M.; Li, X.; Hratchian, H. P.; Izmaylov, A. F.; Bloino, J.; Zheng, G.; Sonnenberg, J. L.; Hada, M.; Ehara, M.; Toyota, K.; Fukuda, R.; Hasegawa, J.; Ishida, M.; Nakajima, T.; Honda, Y.; Kitao, O.; Nakai, H.; Vreven, T.; Montgomery, J. A., Jr.; Peralta, J. E.; Ogliaro, F.; Bearpark, M. J.; Heyd, J.; Brothers, E. N.; Kudin, K. N.; Staroverov, V. N.; Kobayashi, R.; Normand, J.; Raghavachari, K.; Rendell, A. P.; Burant, J. C.; Iyengar, S. S.; Tomasi, J.; Cossi, M.; Rega, N.; Millam, N. J.; Klene, M.; Knox, J. E.; Cross, J. B.; Bakken, V.; Adamo, C.; Jaramillo, J.; Gomperts, R.; Stratmann, R. E.; Yazyev, O.; Austin, A. J.; Cammi, R.; Pomelli, C.; Ochterski, J. W.; Martin, R. L.; Morokuma, K.; Zakrzewski, V. G.; Voth, G. A.; Salvador, P.; Dannenberg, J. J.; Dapprich, S.; Daniels, A. D.; Farkas, O¨.; Foresman, J. B.; Ortiz, J. V.; Cioslowski, J.; Fox, D. J. Gaussian 09, Revision E.01; Gaussian, Inc.: Wallingford, CT, 2009.